This dissertation has been
microfilmed exactly as received 68-725

MERLISS, Frederick E., 1925-
MOLECULAR DIFFUSION COEFFICIENTS IN AQUEOUS BINARY SOLUTIONS.

The University of Oklahoma, Ph.D., 1968
Engineering, chemical

University Microfilms, Inc., Ann Arbor, Michigan

Downloaded from SHAREOK. Persistent Handle URL: https://hdl.handle.net/11244/2291

THE UNIVERSITY OF OKLAHOMA

GRADUATE COLLEGE

MOLECULAR DIFFUSION COEFFICIENTS IN AQUEOUS BINARY SOLUTIONS

A DISSERTATION

SUBMITTED TO THE GRADUATE FACULTY

in partial fulfillment of the requirements for the

degree of

DOCTOR OF PHILOSOPHY

BY

FREDERICK E. MERLISS

Norman, Oklahoma

1967

MOLECULAR DIFFUSION COEFFICIENTS IN

AQUEOUS BINARY SOLUTIONS

APPROVED BY

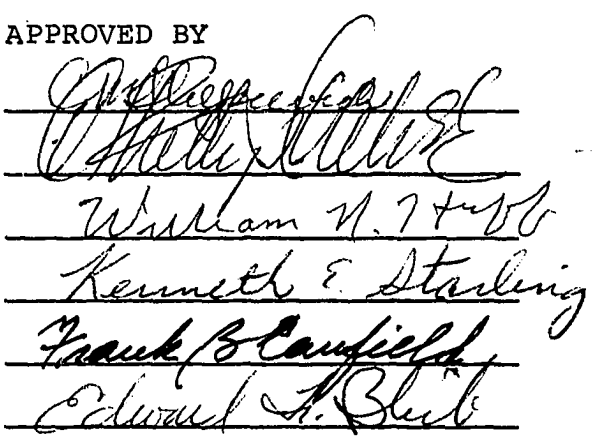

ACKNOWLEDGMENTS

Without the assistance of a number of people the completion of this research would never have become a reality. Among those who have contributed to this work the following persons deserve both special recognition and gratitude:

Dr. C. Phillip Colver, Assistant Professor of Chemical Engineering, for his direction and support during the experimental and final stages of this research.

Mr. James C. Hood, Supervisor of the Physics Instrument Shop, for his assistance in the design of the diffusion test cell and lens mounts, and for the many overtime hours he spent on the construction of the interferometer components and experimental apparatus.

Mr. Harry H. West, a fellow graduate student, for his valuable assistance in much of the mathematical analyses of the experimental data.

Dr. Frank B. Canfield, Associate Professor of Chemical Engineering, and Dr. Kenneth E. Starling, Assistant Professor of Chemical Engineering, for their many helpful suggestions on and discussions of this research.

Finally, I am most grateful to Dr. Cedomir M. Sliepcevich, Research Professor of Engineering, without whose encouragement and assistance I would not have been

able to leave industry to return to graduate school.

In conclusion, I am grateful to the various organizations who have provided partial financial assistance over the course of this research and wish to acknowledge their support. Among these are:

The National Aeronautics and Space Administration who provided a fellowship for personal support and also provided a portion of the experimental equipment.

The National Science Foundation who provided funds for the construction of the major part of the experimental apparatus and for operating expenses under Research Grant No. GK-1023.

ABSTRACT

An apparatus, consisting of a birefringent interferometer, a constant temperature air bath with controls, and a diffusion test cell, was constructed for the purpose of measuring molecular diffusion coefficients of aqueous binary solutions. The interferometer design was essentially that of Bryngdahl with a number of modifications to allow for greater flexibility and more ease of alignment.

Sucrose-water and triethylene glycol-water systems were investigated.

Diffusion coefficients for the sucrose-water system compared to those of Akeley and Gosting to within two percent.

For the triethylene glycol-water system, diffusion coefficients were determined as a function of composition at temperatures of 30°C, 45°C, and 60°C. Coefficients determined for this system were compared to a number of frequently used correlations. For very low triethylene glycol concentrations at 30°C the correlation of Othmer and Thakar predicts a diffusion coefficient within five percent of those determined experimentally. For very low water concentrations at 30°C, only the correlation of Wilke and Chang predicts a coefficient to within 25 percent of the experimental coefficient. At intermediate

concentrations, an empirical correlation proposed by Rathbun predicts the experimental data to within five percent at all temperatures.

TABLE OF CONTENTS

		Page
LIST OF TABLES		viii
LIST OF ILLUSTRATIONS		ix
Chapter		
I.	INTRODUCTION	1
II.	LITERATURE REVIEW	5
III.	EXPERIMENTAL EQUIPMENT AND PROCEDURES	30
IV.	EXPERIMENTAL RESULTS	82
V.	CONCLUSIONS AND RECOMMENDATIONS	91
LITERATURE CITED		95
APPENDICES		
A.	NOMENCLATURE	99
B.	MATHEMATICAL DERIVATIONS	103
C.	GRAPHS OF CALCULATED DATA	107

LIST OF TABLES

Table		Page
1.	Mutual Diffusion Coefficients, Sucrose-Water System	84
2.	Mutual Diffusion Coefficients, Triethylene Glycol-Water System	86

LIST OF ILLUSTRATIONS

Figure		Page
1.	Photograph of the Experimental Apparatus	31
2.	Photograph of the Laser and Beam Diverging Lens Mount	32
3.	Interferometer Lens and Window Arrangement	36
4.	Photograph of Savart Plate Mount	37
5.	Photograph of Assembled Diffusion Test Cell	42
6.	Schematic Drawing of the Diffusion Test Cell	43
7.	Photograph of Fluid Holding Reservoir	46
8.	Schematic Diagram of Constant Temperature Air Bath	50
9.	Wiring Diagram of the Control Heater Circuit	53
10.	Wiring Diagram of the Auxiliary Heater Circuit	54
11.	Deviation of Temperature from the Set Point During Experimental Run Number A-TEG-17	67
12.	Determination of the Diffusion Coefficient from D'_{AB} and θ for 0.1 Weight Percent Aqueous Sucrose Solution	108
13.	Determination of the Diffusion Coefficient from D'_{AB} and θ for 0.5 Weight Percent Triethylene Glycol-Water Solution	109
14.	Determination of the Diffusion Coefficient from D'_{AB} and θ for 34 Weight Percent Triethylene Glycol-Water Solution	110

Figure Page

15. Determination of the Diffusion Coefficient from D'_{AB} and θ for 67 Weight Percent Triethylene Glycol-Water Solution 111

16. Determination of the Diffusion Coefficient from D'_{AB} and θ for 99.5 Weight Percent Triethylene Glycol-Water Solution 112

17. Mathematical Representation of Interference Pattern Showing Measurements Made on Actual Patterns 78

18. Interference Patterns for Various Times During Experimental Run Number 1-S-2 81

19. Molecular Diffusion Coefficients for the Triethylene Glycol-Water System as a Function of Composition and Temperature . . . 85

20. Comparison of Experimental Values of Diffusion Coefficients for the Triethylene Glycol-Water System to Predicted Values by Equation (42) 90

MOLECULAR DIFFUSION COEFFICIENTS IN AQUEOUS BINARY SOLUTIONS

CHAPTER I

INTRODUCTION

Numerous chemical processes are involved with mass transport. The design of equipment for carrying out these processes in either the laboratory or in commercial scale plants depends upon a knowledge of mass transport coefficients. Mass transport coefficients in turn are dependent upon molecular diffusion coefficients.

Molecular diffusion in fluids may be defined as the dissipation of concentration irregularities by molecular movement in the absence of gravitational, momentum and thermal gradients. When two or more fluids, at least partially miscible, are juxtaposed under such conditions that only concentration gradients exist in the system, the fluids begin to diffuse into each other. The diffusion will continue until the system attains thermodynamic equilibrium.

In 1850, Graham published results of what is believed to be the first large scale investigation of molecular diffusion in liquids (27). His results, although intriguing, shed little light upon the diffusion process.

In 1855, Adolph Fick, a German doctor of medicine, undertook a study of molecular diffusion with the express purpose of determining the fundamental law which governs the diffusion process (17). Although Fick was unsuccessful in his pursuit of the determination of the fundamental law of diffusion, he postulated an equivalence between molecular transport by diffusion and thermal transport by conduction. Thus Fick laid the foundation for study of the molecular transport of matter.

Consequently, two laws of molecular diffusion are attributed to Fick, and bear his name. The first law defines a coefficient for molecular diffusion as the proportionality constant necessary to equilibrate the flux of a species in a binary system to the concentration gradient of that species in the system. Mathematically this may be stated as

$$J_A = -D_{AB} \text{ grad } C_A \qquad (1)$$

where J_A and grad C_A are respectively the flux of species A relative to a fixed coordinate system and the gradient of species A in the binary system composed of species A and B. The flux of the species is defined as the amount of matter diffusing, in the direction of the concentration gradient, through a unit area per unit of time. The negative sign results because the diffusion occurs in a direction opposite to that of increasing concentration gradient. D_{AB} is the mutual molecular diffusion coefficient of species A in species B.

The second law of Fick is derived from considerations of transient or unsteady state diffusion. Tyrell (64) made a study of Fick's work and concluded that Fick considered the important contribution of his work to be the differential equation, now known as Fick's second law,

$$\frac{\partial C_A}{\partial t} = \text{div } (D_{AB} \text{ grad } C_A) \qquad (2)$$

where t is time and the other terms have the same meaning as for equation (1).

Since publication of Fick's original manuscripts, a great deal of work and study has been undertaken to determine the molecular diffusion coefficient, D_{AB}, from theoretical considerations.

As is to be expected, the theory of molecular diffusion for the gaseous state is relatively well developed in comparison to that for the liquid state. This, in part, results from the fact that the kinetic theory of the gaseous state is relatively well defined, while there is presently no workable kinetic theory for the liquid state (42). Even so, predicted values for molecular diffusion coefficients in binary gaseous systems, determined by correlations which have been developed from theoretical considerations, contain significant uncertainties and typically deviate from experimentally determined values by 5 to 10 percent at ambient conditions. Often greater deviations are encountered and for pressures in excess of 20 atmospheres, at or below

normal temperatures, these correlations fail to yield even reasonable estimates for the binary molecular diffusion coefficients (55). No single correlation of gaseous diffusion coefficients has been found to be superior over other correlations for all gaseous systems.

Since there is presently no workable kinetic theory of the liquid state, much less has been accomplished theoretically for the liquid state than for the gaseous state. Even for simple binary liquid systems, no widely applicable molecular diffusion coefficient correlations have been derived from theoretical considerations. However, a large number of correlations have been presented in the literature. These correlations range from being purely empirical to being semitheoretical in nature.

There is a great need for accurate binary molecular diffusion data to test these correlations under a variety of conditions and to improve the quality of the correlations. To the present time there are relatively few data available for this purpose.

The objectives of this research were to build an experimental apparatus from which accurate diffusion data could be obtained and to determine molecular diffusion coefficients at various temperatures and fluid compositions for an aqueous binary liquid system using this apparatus. These objectives have been accomplished.

CHAPTER II

LITERATURE REVIEW

Fick's First and Second Laws

In mathematical descriptions of mass diffusion processes, the assumption is made that linear homogeneous relationships exist between the mass fluxes and the driving forces tending to cause mass movement. According to Fick's first law

$$J_A = -D_{AB} \nabla C_A \qquad (3)$$

the driving force for molecular diffusion is concentration gradient.

Concentrations of the species of the diffusion system may be expressed in a number of different ways. The four most prominent and useful ways are:

(1) mass concentration, ρ_i, - the mass of species i per unit volume of solution,

(2) molar concentration, C_i, - the moles of species i per unit volume of solution,

(3) mass fraction, ω_i - the mass concentration of species i divided by the total mass concentration, ρ, of the system,

and (4) mole fraction, X_i, - the molar concentration of species i divided by the total molar concentration, C, of the solution.

Useful relations among the different expressions for concentrations of the various species in an n component system are:

$$\rho = \sum_{i=1}^{n} \rho_i \tag{4}$$

$$C_i = \rho_i / M_i \tag{5}$$

$$C = \sum_{i=1}^{n} C_i \tag{6}$$

$$\omega_i = \rho_i / \rho \tag{7}$$

$$X_i = C_i / C \tag{8}$$

$$\sum_{i=1}^{n} X_i = \sum_{i=1}^{n} \omega_i = 1 \quad . \tag{9}$$

To complete the mathematical description of molecular diffusion, a frame of reference must be chosen. Each species of the diffusing system travels at a different velocity through the system. By denoting the average molecular velocity of species i, relative to fixed coordinate axes, as u_i, the local mass average velocity in an n component system is defined by

$$u^m = \sum_{i=1}^{n} \rho_i u_i / \sum_{i=1}^{n} \rho_i \quad . \tag{10}$$

In a like manner the local molar average velocity is defined by

$$u^M = \sum_{i=1}^{n} C_i u_i / \sum_{i=1}^{n} C_i \quad . \tag{11}$$

Choosing the reference frame as the local average velocity, the diffusion velocity of species i relative to the local average velocity is then defined as $u_i - u^m$ or $u_i - u^M$, depending on whether mass units or molar units are chosen for the system. Ordinarily it is expedient to employ molar units; therefore the remainder of this discussion will be restricted to molar units, and will, also, be restricted to a binary system.

Now that a reference frame has been selected, the diffusion flux of component A of the binary system AB may be written as

$$J_A^M = C_A \, (u_A - u^M) \tag{12}$$

$$\underset{\text{(total flux)}}{C_A u_A} = \underset{\text{(diffusional flux)}}{J_A^M} + \underset{\text{(convection flux)}}{C_A u^M} \quad . \tag{13}$$

In equations (12) and (13) the diffusional flux is defined by Fick's first law as

$$J_A^M = -D_{AB}^M \nabla C_A \quad . \tag{14}$$

The equivalent equations for component B are

$$C_B u_B = J_B^M + C_B u^M \tag{15}$$

and

$$J_B^M = -D_{BA}^M \nabla C_B \quad . \tag{16}$$

Equations (14) and (16) serve to define the diffusion coefficients D_{AB}^M and D_{BA}^M. The continuity equations for components A and B are

$$\frac{\partial C_A}{\partial t} = - \nabla \cdot (J_A^M + C_A u^M) \tag{17}$$

and

$$\frac{\partial C_B}{\partial t} = - \nabla \cdot (J_B^M + C_B u^M) \quad . \tag{18}$$

Obviously equations (17) and (18) reduce to Fick's second law equations

$$\frac{\partial C_A}{\partial t} = - \nabla \cdot J_A^M \tag{19}$$

and

$$\frac{\partial C_B}{\partial t} = - \nabla \cdot J_B^M \tag{20}$$

if and only if u^M goes to zero. Generally, the experimentalist can choose conditions such that u^M is sufficiently small to be neglected (4, 26).

By use of equations (6) and (11) it is seen on addition of equations (13) and (15) that

$$J_A^M + J_B^M = 0 \quad . \tag{21}$$

An analysis shows that if u^M is negligible or zero that C in equation (6) and the molar volume of the system AB must be constant. In other words C must be independent of composition in the system AB. Therefore,

$$\nabla C_A + \nabla C_B = 0 \tag{22}$$

and

$$D_{AB}^M = D_{BA}^M \quad . \tag{23}$$

Generally it is accepted that Fick's second law for one dimensional diffusion in a stationary binary liquid system with no chemical reaction and no volume changes on mixing may be written as

$$\frac{\partial C_A}{\partial t} = \frac{\partial}{\partial \xi} \left(D_{AB} \frac{\partial C_A}{\partial \xi} \right) \tag{24}$$

for component A (or B with proper subscripts). However, an additional restriction, that the partial molal volumes of the two components of the binary system be constant and equal, is necessary if equations (10) and (20) or equation (23) are to hold absolutely.

Further analysis of Fick's first and second law equations yields a diffusion coefficient, on the basis of mass units D_{AB}^{m}. It has been shown in the literature (6, 63) that for binary diffusion

$$D_{AB}^{M} = D_{AB}^{m} \quad . \tag{25}$$

Therefore, the diffusion coefficient for binary systems is referred to as the mutual diffusion coefficient D_{AB} without use of superscripts (7).

Correlations of Diffusion Coefficients

Much work, performed over many years, has been directed toward relating molecular diffusion coefficients to physical, chemical and thermodynamic properties of the constituents in the diffusing system. The goals of this work are to obtain accurate methods of predicting molecular diffusion coefficients.

Early work toward determining methods of predicting diffusion in gaseous mixtures centered on semitheoretical and empirical correlations of diffusion coefficients. Considerable has been accomplished in recent years, through the use of the kinetic theory of gases and modern mathematical

theory of non-uniform gases, to derive theoretical expressions for predicting binary diffusion coefficients for gaseous systems. For the most part, results obtained from these recent studies have supplanted the earlier correlation schemes.

However, even for gases there is much concern as to how the phenomenological functions in the theoretical equations should be evaluated. The evaluation of all such functions is at least partially empirical. Consequently, there have been a large number of correlations derived using various simplifications of the phenomenological functions. At best, the presently available correlations are only applicable within about ten percent.

Extension of the correlations which have been developed for diffusion in binary gas mixtures to multicomponent gas mixtures is complex. It depends upon both the geometry of the system and boundary conditions for the system. Ordinarily the equations written to describe multicomponent molecular diffusion in gaseous systems involve the binary molecular diffusion coefficients to represent the molecular properties of the gaseous system. Hirschfelder, Curtis, and Bird (31) give the basic theory of diffusion in multicomponent gaseous systems.

Liquid state theory is only partially developed. Existing theories are not sufficiently sound to provide a good basis for prediction of molecular diffusion coefficients. Therefore, in contrast to theoretical methods used in

predicting gaseous diffusion coefficients, empirical equations are used to predict molecular diffusion coefficients for liquid systems.

Due to the wide variety of liquid systems that may be encountered, a number of the empirical equations are used depending upon the nature and chemical characteristics of both solvent and solute in the liquid system under consideration. The basis for study of electrolytic solutions is quite different from that for non electrolytes. The following will be restricted to discussion of the more prominent empirical equations for predicting molecular diffusion in nonelectrolytic binary liquid systems. Most of these equations have been tested sufficiently against experimental data that their general limitations are known. In these equations the first subscript on the diffusion coefficient will represent the solute and the second represents the solvent.

Molecular diffusion coefficients in liquid systems are much more concentration dependent than are those for gaseous systems. There has been little or no success in attempts that have been made to generalize the available empirical equations to predict concentration dependence of diffusion coefficients. As a result it is necessary to consider one type of equation for prediction of diffusion coefficients in dilute solutions and a completely different type for the prediction of concentration dependence of diffusion coefficients.

The Stokes-Einstein equation (also attributed to Nernst and to Sutherland)

$$D_{AB} = \frac{kT}{6\pi\mu b} \tag{26}$$

is basic to the development of most of the empirical equations for predicting dilute solution diffusion coefficients. This expression was derived from hydrodynamic considerations for very dilute solutions of a species of large spherical molecules of radius b diffusing through a solvent of small molecules, having viscosity μ, which appears as a continuum to the large diffusing particles. This equation fails to give even reasonable estimates of the diffusion coefficient when the size of the solute molecules approaches the size of the solvent molecules.

Polson (53), by making a number of approximating assumptions to evaluate the radius of the large molecules, reduced equation (26) to

$$D_{AB} = 2.74 \times 10^{-5} M_A^{-1/3} \tag{27}$$

for large unhydrated molecules diffusing in water at room temperature. He found substantial agreement with experimental data when M_A, the molecular weight of the dilute component, is greater than 1000.

Generally the Stokes-Einstein equation is used for estimating the effect of small temperature changes on D_{AB}

by assuming the radius of the molecules of the dilute component to be unaffected by the temperature change. Thus when D_{AB} at T_1 is known D_{AB} at T_2 is

$$D_{AB}(T_2) = D_{AB}(T_1)\left[\frac{T_2\mu(T_1)}{T_1\mu(T_2)}\right] . \qquad (28)$$

However, Innes and Albright (34) show this to be a weak approximation. Othmer and Thakar (51) found for a number of systems that the viscosity ratio in equation (28) should be raised to the 1.1 power for more realistic estimates.

The Wilke-Chang equation

$$D_{AB} = 7.4 \times 10^{-8}[(\Phi M_B)^{1/2}\, T/\mu_B \underline{V}_A^{0.6}] \qquad (29)$$

incorporates an association parameter, Φ, for the solvent, and the molal volume $\underline{V}_A$ of the solute. The molal volume of the solute is measured at the normal boiling point of the solute. Values of Φ for several solvents are tabulated in the literature (66). Estimates of diffusion coefficients from equation (29) are usually high by a factor of about 2.3. However, this equation is recommended for estimating diffusion coefficients for dilute solutions of water in organic solvents if the results are divided by 2.3 (55).

The Scheibel equation

$$D_{AB} = \frac{KT}{\mu_B \underline{V}_A^{1/3}} \qquad (30)$$

is a modification of the Wilke-Chang equation with the elimination of the association parameter Φ. The constant, K, in equation (30) is evaluated from

$$K = 8.2 \times 10^{-8} \ (1 + 3\underline{V}_B/\underline{V}_A)^{2/3} \qquad (31)$$

with various restrictions placed on the value that should be used for the ratio $\underline{V}_B/\underline{V}_A$. For different solvents, values of K to be used are tabulated (56). The molal volumes, $\underline{V}_B$ and $\underline{V}_A$, are to be measured at the normal boiling point. This equation has not proved to be as reliable as the Wilke-Chang relationship.

Othmer and Thakar observed for a large number of systems that log D_{AB} is essentially linear in log μ_B for a given binary diffusion system as temperature is varied. The slope of the line is the ratio of activation energies for diffusion and viscosity. Starting from this, the relationship

$$D_{AB} = 14.0 \times 10^{-5} \left(\underline{V}_1^{0.6} \mu_B \mu_W^{1.1\Delta H_B/\Delta H_W} \right)^{-1} \qquad (32)$$

was developed, where ΔH_B and ΔH_W are the latent heats of vaporization for the solvent and water respectively at the temperature of interest. This amounts to substituting $\mu_W^{-1.1\Delta H_B/\Delta H_W}$ for $(\Phi M_B)^{1/2}T$ in the Wilke-Chang equation. For 76 systems between 7 and 25°C, this equation yielded predictions within plus or minus thirteen percent of

experimentally determined diffusion coefficients. However, for an aqueous solvent the average deviation was about five percent. Therefore the Othmer-Thakar relationship is recommended for dilute aqueous systems. For these systems equation (32) becomes

$$D_{AB} = 14.0 \times 10^{-5} \mu_W^{-1.1} \underline{V}_A^{-0.6} \quad . \tag{33}$$

Of more recent vintage is the relationship of Gainer and Metzner (19). Beginning with Eyring's absolute reaction rate theory they arrived at the Eyring (22) equation

$$D_{AB} = \frac{kT}{\delta \mu_B} \left(\frac{N_o}{\underline{V}_B} \right)^{1/3} \exp \left(\frac{E_{\mu,B} - E_{D,AB}}{RT} \right) \tag{34}$$

where N_o is Avogadros number and $E_{\mu,B}$ and $E_{D,AB}$ are the activation energies for viscosity and diffusion for the system. δ is a parameter which describes the geometrical configuration of the diffusing molecule and its neighbors. Eyring and co-workers had previously assumed, for lack of better information, that

$$E_{\mu,B} - E_{D,AB} = 0 \quad . \tag{35}$$

Gainer and Metzner offer means for calculating the activation energies individually to evaluate the expression. The Eyring assumption is reputed to be sound for self diffusion which allows the determination of δ from self diffusion

data. The method used to evaluate the activation energies is quite complex. The results obtained from equation (34) using activation energies calculated by the proposed method deviate on the average by about 18 per cent from experimental values. Thus other empirical equations offer better estimates of diffusion coefficients. Further work is being done on this approach.

Bearman (5) presents a sophisticated approach to the problem of relating molecular friction to properties of liquids through statistical mechanical theory. Presently his developments are restricted to regular solutions of molecules having similar sizes, shapes, and interaction potentials. Bearman shows that statistical mechanical theory and the theories of Eyring and of Hartley and Crank (30) relate mutual and self diffusion coefficients by equations of the same form. Although promising this theory is not yet sufficiently developed to predict diffusion coefficients.

However, Kamal and Canjar (36, 37) on the basis of statistical mechanical theory have developed an expression for D_{AB} of the form

$$D_{AB} = K_1 K_2 \qquad (36)$$

and have tabulated values of K_1 and K_2 for a number of binary systems. For about 50 systems it has proved to be almost as reliable as the Wilke-Chang equation but it suffers from complexities in the determination of the values K_1 and K_2.

To evaluate these functions one needs to know the value of the ratio of total volume to volume occupied by the molecules in the system. This must be obtained from measurements of the velocity of sound through the liquid or other suitable means. This relation is interesting because at infinite dilution it depends only upon a product of two quantities, one which involves properties of solvent only and the other which involves properties of solute only. Dependence of K_1 and K_2 on temperature is very complicated. Therefore it is difficult to use this equation at temperatures other than that for which values of the functions are tabulated.

In general, the equations developed for estimating dilute solution diffusion coefficients are not accurate to better than ten percent. Most predict values for diffusion coefficients which are higher than those measured experimentally. However, much of the data in the literature by which these correlations were tested are probably not more accurate than ten percent. Recently published data is most accurate but is not available in the abundance required to fully test these correlations.

There are several correlations for predicting the effect of concentration on diffusion coefficients. Their general forms are similar, but some involve infinite dilution diffusion coefficients, some self diffusion coefficients, and some involve tracer diffusion coefficients.

Infinite dilution diffusion coefficients are defined as

$$\overline{D}_{AB}^{\infty} = \underset{C_A \to 0}{\text{limit}} \; D_{AB} \quad . \tag{37}$$

Self diffusion coefficients, D_{AA} and D_{BB}, are defined as the diffusion through a system of a trace of a substance identical, except for some trivial characteristic, with either component A or B respectively.

There are two types of tracer diffusion coefficients. The first type is a measured coefficient obtained by tagging a small number of molecules of a substance with a radioactive tracer and measuring the diffusion of these molecules through a solvent of untagged molecules of the same substance. These coefficients should be identical to self diffusion coefficients.

The second type is also a measured coefficient obtained by tagging a small number of molecules of a substance with a radioactive tracer and measuring the diffusion of these molecules through a solvent of untagged molecules of the other component of the binary system being studied. This coefficient has been found to be dependent on the concentration of the tagged molecules. However, in the limit as the concentration of tagged molecules goes to zero this type of tracer diffusion coefficient should be the infinite dilution diffusion coefficient of the binary system.

Nagarajan, Ryan and Shemilt give the correlation

$$D_{AB}^{*} = 1.39 \times 10^{-7}/\mu_B \tag{38}$$

for tracer diffusion coefficients of the second type. Equation (38) showed an excellent correlation for ten different liquids for temperature variations between 0 and 55°C.

Many non polar solutions approach being regular. For regular solutions, with the additional restriction of additive volumes, Bearman, using statistical mechanical theory, developed the relation

$$D_{AB}(C) = (D^{\infty}_{BA}X_A + D^{\infty}_{AB}X_B)\frac{\partial \ln a_A}{\partial \ln X_A} \quad . \qquad (39)$$

This equation, however, was originally proposed by Darken (16) on an empirical basis, where D^{∞}_{BA} and D^{∞}_{AB} are replaced by D_{BB} and D_{AA} respectively.

In Bearmans derivation the assumption is made that

$$\frac{D_{AA}}{D_{BB}} = \frac{\bar{V}_B}{\bar{V}_A} \quad . \qquad (40)$$

He shows that the self diffusion coefficient D_{AA} should be interchangeable with the infinite dilution diffusion coefficient D^{∞}_{BA}.

For ideal solutions

$$\frac{\partial \ln a_A}{\partial \ln X_A} = 1 \qquad (41)$$

so that equation (30) may be considered as yielding a binary

diffusion coefficient by correction of an ideal solution diffusion coefficient with a thermodynamic factor. It has been found by several investigators (54, 63) that equation (30) tends, in most systems, to overcorrect for lack of ideality.

For certain systems tested by Rathbun (54) it was determined that an equation of the form

$$D_{AB}(C) = (D^{\infty}_{BA}X_A + D^{\infty}_{AB}X_B)\left(\frac{\partial \ln a_A}{\partial \ln X_A}\right)^S \qquad (42)$$

would satisfactorily correlate the data. For systems having positive deviation from Raoult's Law the value of S used was 0.6. For systems exhibiting negative deviation from Raoult's law S was taken as 0.3. Rathbun tested solutions composed of one associating component and one nonassociating component. His correlation derives from a purely empirical fit of data on the systems tested. Equation (42) has not been sufficiently tested to determine any uniqueness to the values of S.

Equation (39) has been found to hold for nearly ideal binary solutions but to be unreliable for highly non-ideal mixtures. Deviations from equation (39) become large where molecular association of either component of the mixture is appreciable.

Only recently Vignes (65), from observation of the curvature of isotherms of binary diffusion coefficients

empirically arrived at the equation

$$D_{AB}(C) = (D_{AB}^{\infty})^{X_B} (D_{BA}^{\infty})^{X_A} \frac{\partial \ln a_A}{\partial \ln X_A} \qquad (43)$$

for correlating binary diffusion data on liquid and solid systems, with the exception of associating mixtures. At the same time, Cullinan (15) beginning with the absolute reaction rate theory based on the "hole model" of Eyring, has derived equation (43) on a semitheoretical basis. Cullinan states that Vignes has shown this correlation to be valid for all binary liquid and solid systems measured to date with the exception of associated mixtures. From analysis of the results presented by Vignes it appears that the correlation may also have some application in associated systems.

Experimental Methods

The design of the experimental system for the determination of diffusion coefficients is dependent upon the means which will be used to analyze the data. The experiments are designed so that the data are taken under conditions which approximate those required for either Fick's "first" or "second law" to apply. The data are then readily interpreted. However, the accuracy of the results depends not only upon the degree of approximation of these conditions but also upon the accuracy of the analytical techniques involved in obtaining the data (21).

In selecting an experimental technique for this research, the various methods that have been used and

discussed in the literature were studied. The most prominent of these are discussed here.

Experimental methods for the determination of diffusion coefficients can be separated into two categories, steady state and unsteady state. Also, under certain circumstances determinations are made in systems where the conditions approximate steady state and as such are called pseudo-steady state determinations. The latter category is made more easily than by other methods but the quality of the results obtained is far from that required to develop quantitative diffusion theory.

The pseudo-steady state methods are exemplified by the porous diaphragm method (24, 50, 58). In this method diffusion occurs as a result of a nearly steady concentration gradient across a porous diaphragm. The diaphragm is composed of sintered glass, porous porcelain or other material inert to the test solutions.

Typically the diaphragm cell is operated in a vertical position, that is, two chambers of equal volume lie one above the other with the diaphragm between. The more dense of the test solutions is admitted to fill the lower chamber and the diaphragm, and the less dense solution is charged to the upper chamber. The concentration gradient is established across the diaphragm by allowing diffusion to proceed for an initial period, usually from two to eight hours. The cell is then emptied and again charged with fresh solution. Diffusion is then allowed to proceed for a known period of time which is

usually from one to three days duration. The diffusion coefficient is obtained from analysis of the solutions made before and after the diffusion period. Based on Fick's "first law," the diffusion coefficient then is calculated from

$$D_{AB} = \frac{1}{\beta \Delta t} \ln \left(\frac{(\Delta C_A)_o}{(\Delta C_A)_t} \right) \qquad (44)$$

where $(\Delta C_A)_o$ is the initial concentration difference between the two solutions and $(\Delta C_A)_t$ is the concentration difference after the elapsed time t. The calibration factor, β, is the cell constant and is determined from measurements made using a solution of known diffusion coefficient (40, 45, 47). The diffusion coefficient so determined represents an average diffusivity over the log mean of concentration difference with time.

There are a number of modifications of this method (1, 40, 47) which are said to improve the results. However, the accuracy of determination of the diffusion coefficient by any of the diaphragm cell methods is only as good as the analytic technique used to determine the concentrations of the two solutions. With precise analysis techniques, these methods are capable of yielding diffusion coefficients accurate to about one percent. But, due to the lengthy time each experiment must operate, a high degree of temperature control is mandatory.

Some steady state methods are accomplished in much the same way. A modified diaphragm cell is usually used in this method. Both solutions are pumped through the chambers of the cell. The least dense of the fluids is circulated through the upper chamber at a sufficiently high rate so that the entrance and exit concentrations differ negligibly. The more dense solution is circulated more slowly through the lower chamber of the cell. The circulation of fluid is continued until the effluent concentration of the more dense fluid remains constant at an incrementally lower level than that of the inlet concentration level. Based on Fick's "first law," the difussion coefficient is determined by

$$D_{AB} = \frac{Q}{\beta V_c} \ln \left\{ \frac{(\Delta C_A)_{in}}{(\Delta C_A)_{out}} \right\} \qquad (45)$$

where V_c is the volume of the lower chamber of the cell, Q is the volumetric flow rate of the more dense fluid, $(\Delta C_A)_{in}$ is the concentration difference between the two solutions at the inlet of the cell and $(\Delta C_A)_{out}$ is the concentration difference at the exit of the cell. The cell constant, β, is determined, as in the diaphragm cell method, by measuring the diffusion of a solution with a known diffusion coefficient. In this method of measurement, diffusion parallel to the direction of flow is neglected. An accuracy of about five percent results from the use of this method. The diffusion coefficients measured represent an average diffusivity over the log mean concentration difference.

The analyses of unsteady state data are based on Fick's "second law" of diffusion and are grouped into two general classes, infinite or free diffusion and restricted diffusion. Restricted diffusion is defined as that mode of diffusion in which the composition changes are appreciable at one or more boundaries of the system. Free diffusion is characterized by constant boundary conditions. One example of restricted diffusion is observed when free diffusion is allowed to proceed for very long times so that appreciable composition changes occur at the boundaries.

In one method of restricted difussion, an initial boundary is formed in a vertical cell between a less dense upper solution and a more dense lower solution. Diffusion between the two solutions is allowed to occur and either the concentration profiles are studied as a function of time, or the upper and lower solutions are separated and analyzed to determine the diffusion coefficient. The best method for analysis for this system is the Harned conductance method (28, 29) and can be applied only to electrolytes with an accuracy up to about 0.2 percent. For nonelectrolytes the best analysis methods available give diffusion coefficients to no better than one percent accuracy, with usual accuracies in the range from 8 to 25 percent.

In free diffusion, as in the method of restricted diffusion discussed, an interface or initial boundary is established between a less dense upper solution and a more dense lower solution. The diffusion coefficient is determined

from measurements of the concentration profiles after diffusion commences. Although the necessary equipment for measuring the concentration profiles is complex, the methods available can yield diffusion coefficients to an extremely high degree of accuracy. Interferometric methods are well suited for such measurements and, among the currently available methods, yield the most accurate data (42). This results in part because there is no need for physical sampling and analysis of the solutions when using interferometry, and consequently, once the concentration profile is established, it is not disturbed during the experiment. Also, use of interferometry is dependent only upon the refractive index differences between the species in the system being measured.

The most serious problem encountered in infinite diffusion studies is the inability to form a sharp initial boundary between the two solutions in the test cell (9, 18, 42, 43). The formation of a sharp initial boundary is sensitive to the concentration difference between the solutions being tested. The smaller the concentration difference the greater is the sensitivity in establishing the initial boundary to the required degree of sharpness. However, there are highly satisfactory means for effecting a suitable initial boundary condition (11, 12, 35, 39, 49, 59). Although these methods do not produce an infinitely sharp initial boundary condition, mathematical techniques have been derived for correcting the measured experimental parameters to account for the imperfection (9, 18, 26, 43).

The analyses of the data to determine the diffusion coefficient in interferometric methods are based upon relationships between the complex mathematics of the optical system of the interferometer, the refractive indices of the test solutions, and the unsteady state mathematical description of the diffusion process. These analyses are well defined and developed for certain experimental conditions that are readily obtainable (10, 14, 25, 38, 44, 52).

There is one factor common to all techniques for experimentally determining diffusion coefficients which is a potential source of error. The actual diffusion coefficient may be a function of concentration while the coefficient determined experimentally is an integral diffusion coefficient. Therefore, the smaller the difference in concentration of the two original solutions the more nearly the determined coefficient will approach the actual coefficient for a particular value of concentration. At the same time, the smaller the difference in concentration of the two original solutions the greater is the need for extreme accuracy in analysis of the solutions. Consequently, methods which require the least number of independent chemical analyses are preferred and are usually more accurate.

In addition to the above described experimental methods for study of diffusion, numerous others are described in the literature. Most are modifications of one or more of those discussed here.

To obtain data of significance, for use in the development of liquid diffusion theory, the most accurate experimental method available must be employed. This is infinite diffusion using interferometric measurement techniques. The interferometric technique of analysis is preferred not only because of its great accuracy but also for its sensitivity and adaptability to a variety of experimental conditions (10, 42).

CHAPTER III

EXPERIMENTAL EQUIPMENT AND PROCEDURES

Experimental Equipment

The experimental equipment consisted of a birefringent interferometer, a constant temperature air bath with controls and recorder, a flowing junction cell, and a 35 mm camera with auxiliary attachments for recording the data. Two views of the experimental apparatus are shown in Figures 1 and 2.

The Interferometer

Among the presently available methods for determining liquid diffusivities, those which employ interferometric techniques of analysis are considered to be capable of the greatest accuracy (10, 26, 42). Several interferometric techniques have been developed and used for this purpose. The selection of the particular technique for use in a liquid diffusion study depends upon what data is desired and the required accuracy of results.

Two basic types of interferometers are most applicable to precision studies of liquid diffusion. The first of these is used to determine concentration profiles as a function of time and the second is for determining concentration

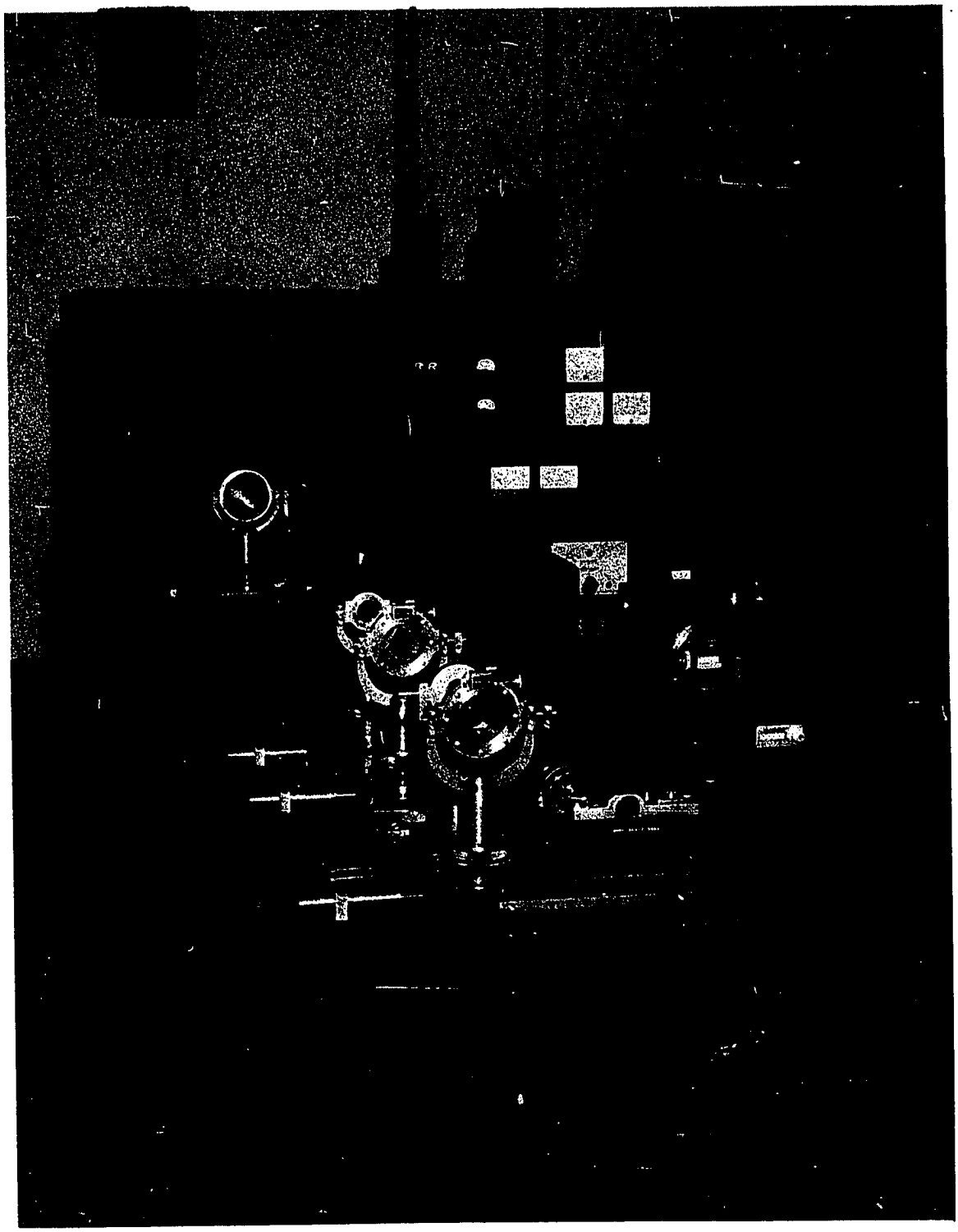

Figure 1. Photograph of the Experimental Apparatus

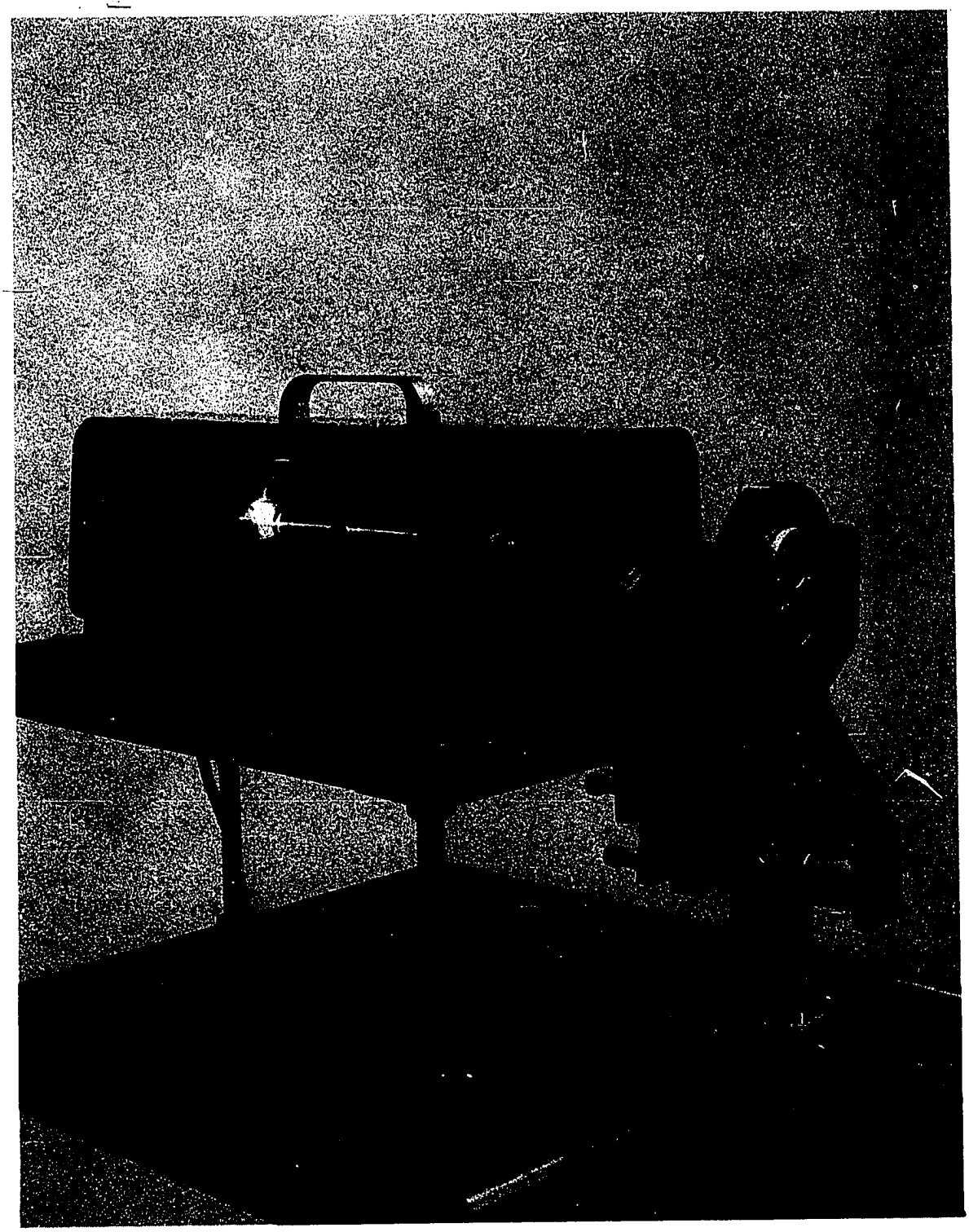

Figure 2. Photograph of the Laser and Beam Diverging Lens Mount

gradients as a function of time. A brief discussion of these two types of interferometers is presented by Lightfoot and Cussler (42). Representative of the first type are the Rayleigh (12) and Mach-Zender (11) interferometers while the Guoy (26) and birefringence interferometers are representative of the second type. However, the birefringence interferometer can also be used to determine concentration profiles as a function of time by minor modification.

Interpretation of data recorded using the first three of the above interferometers depends upon measuring the movement of interference fringes as a function of time. The birefringence type gives a direct representation of the concentration gradient in the diffusing system and also directly records the cell geometry. After an analysis was made of the various types of interferometers, use of the birefringence type, first introduced by Inglestam (32, 33), was selected for the present study. Comprehensive analyses of the birefringence interferometer, including its advantages and limitations, are given by Bryngdahl and Ljunggren (10).

The basic design of the interferometer used was that of the Inglestam (32,33) and Bryngdahl (8). However, a number of modifications were made in the basic design to increase the alignment sensitivity of the instrument.

The interferometer consists of an optical bench, lens system, and polarized laser light source. In Bryngdahl's design the optical bench was approximately ten feet in length. In this work the optical bench was built 20 feet

in length to allow the use of long focal length lenses, and thereby improve the quality of the collimated light beam attainable through the section of the interferometer where the test cell was located. The interferometer optical bench was constructed of two 8-inch steel channels, 20 feet in length, spaced 16 inches apart with 1/4-inch by 3-inch by 16-inch steel plates bolted onto the channels. The channel was supported at its midpoint and at points 3 feet from each end to assure a uniform loading distribution. The supports were concrete pillars with integral bolts used to level the optical bench. Base area of each of the pillars was 264 square inches. The pillars were set on 3/4-inch thick sheets of silicone sponge rubber, COHRlastic R-10470 (Connecticut Hard Rubber Company), in order to absorb vibration. Total weight of the system was approximately 2,400 pounds (including the pillars), thus resulting in a loading on the pads of only about 3 pounds per square inch. Maximum compression of the sponge rubber required 18.5 psi and the compression was specified to be linear with loading for this rubber. Thus this load was only about 1/6 of the total allowable compressive load on the vibration pads.

Each of the optical components of the interferometer including five lenses, two Savart plates, the laser and camera was mounted in an individual mount on the optical bench. Each lens mount was affixed to a magnesium base plate 1 1/2 inches thick, 7 3/4 inches wide and 16 1/2

inches long. Corners of the base plate were drilled and tapped for 1/2 inch threaded rod for attaching the lens mount to the optical bench. The mounts were designed to give maximum flexibility for alignment purposes. They were constructed by the University Physics shop.

Each mount had at least four degrees of freedom of movement and in some cases as many as five degrees of freedom of movement. For each degree of freedom the control on lens movement was to within 0.002 inches. Figure 3 is a schematic representation of the arrangement of the optical components of the interferometer. It also shows the allowable movements for the various mounts for the lenses and Savart plates. A close-up view of one of the Savart plate mounts is shown in Figure 4. This mount is typical of the lens mounts constructed for the interferometer.

The entire system, with the exception of the brass components of the lens mounts and the optical components, was painted with a flat optical black paint to minimize reflections of light in the system.

High quality achromatic lenses were used throughout the system. Lens diameters and focal lengths are given on Figure 3. The Savart plates each consisted of two quartz crystals, 1 1/2 inches square-10 mm thick, cemented together with their optical axes rotated 90° relative to each other. Surfaces of these plates were flat to 200 angstroms or less and were parallel within 15 seconds. All of the optical components were purchased from Karl Lambrecht D/B/A Crystal Optics, Chicago, Illinois.

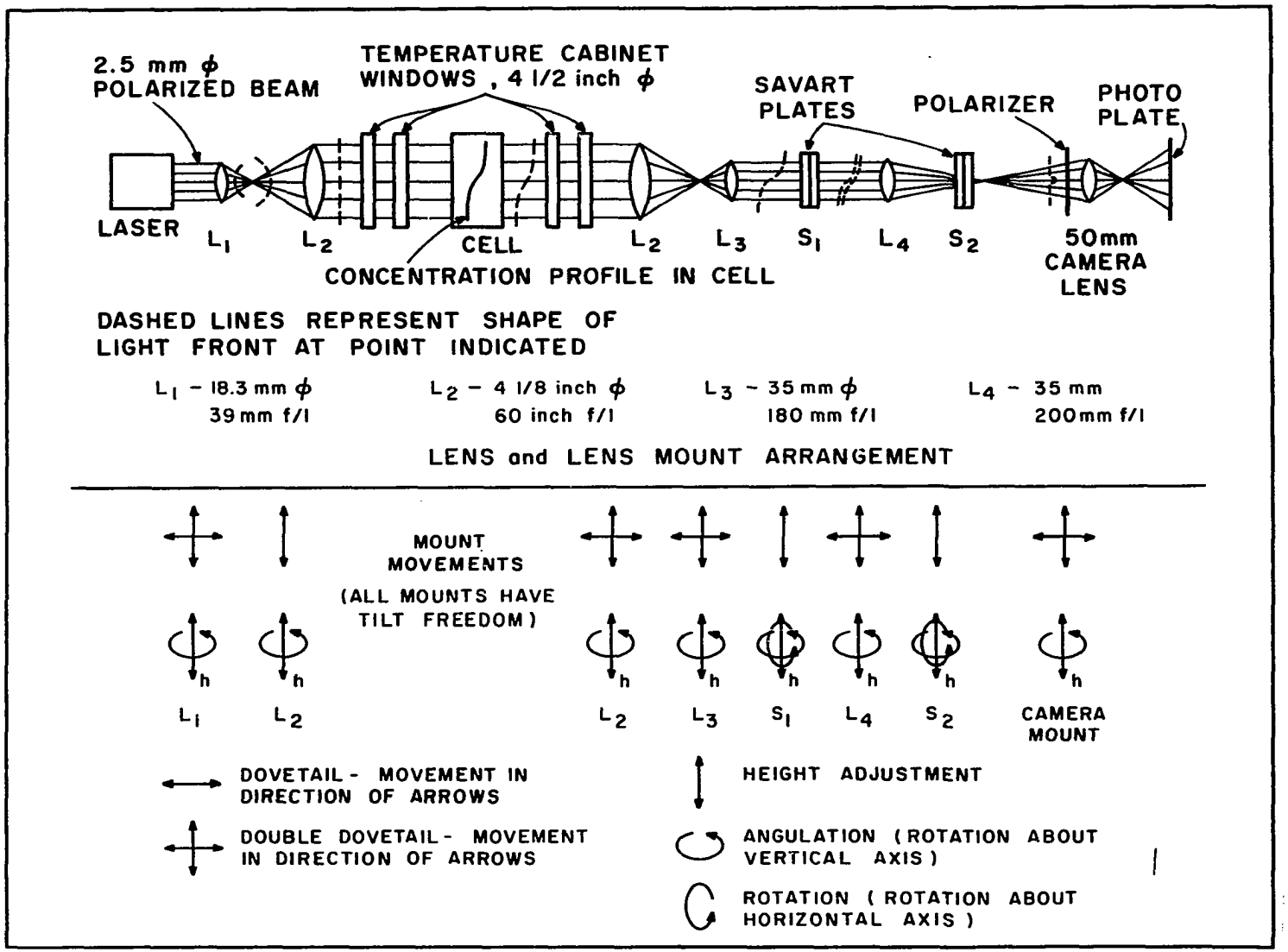

Figure 3. Interferometer Lens and Window Arrangement

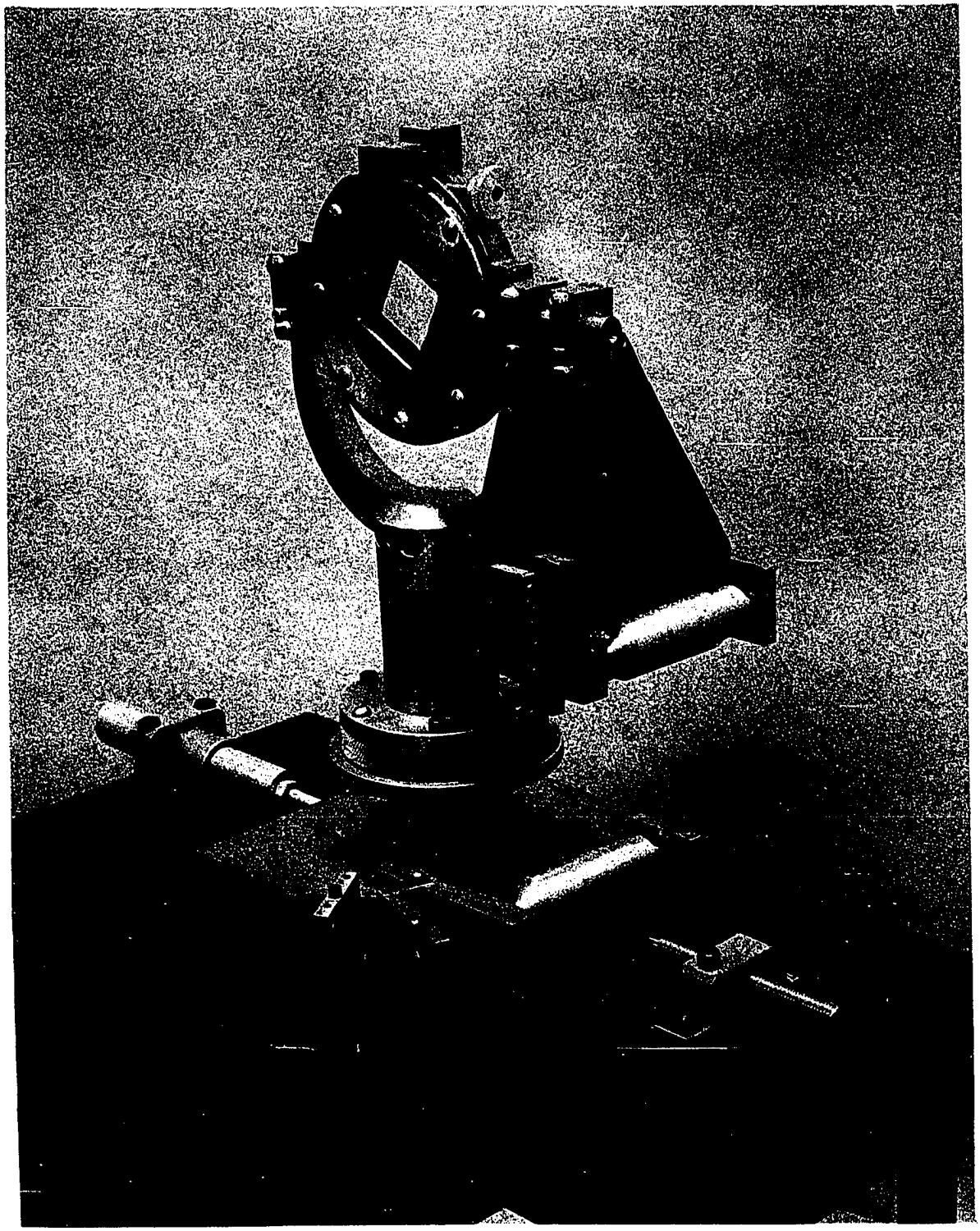

Figure 4. Photograph of Savart Plate Mount

The laser light source (Electro Optics Assoc. LAS-201) had a 1-milliwatt output of collimated polarized light 2.5 mm in diameter. This beam was expanded to a diameter of 4 inches and recollimated to pass through the test cell. After passing through the test cell the beam was reconverged to a diameter of about 12 mm and was recollimated for passage through the first Savart plate. Then the beam was converged through the second Savart plate and fed to the camera lens. By adjustment of the camera lens the beam was focused onto the film plane of the camera where the interference pattern was recorded. A Nikkormat FT 35 mm camera with a 50 mm f.2 lens and a Vemar polarizing filter was used. A bellows attachment and set of extension rings were used to attain sufficient enlargement of the image to observe visually the changes of interference pattern with time.

The laser was 15 inches long, 4 3/4 inches wide and 5 inches high. It was mounted on slide bars on a 1/2 inch thick magnesium plate 15 1/2 inches long by 12 inches wide. The magnesium plate was affixed to the optical bench on a tripod arrangement, which allowed raising, lowering and tilting of the laser. Controlled movement of the laser in a horizontal direction across the magnesium plate was accomplished by adjustment of the slide bars at each end of the laser. About 10° of rotation of the laser, in the plane of the magnesium plate, could also be accomplished by slide bar adjustment.

The laser was a continuous wave helium-neon gas laser. It operated on 118 volt, 60 cycle AC and required a 50 volt-amp power supply. The output beam had a 6328Å wave length in the red region. To maintain a stable output from the laser it was necessary to maintain a constant supply voltage within 1% of the rated voltage. A Sola sinusoidal voltage regulator, rated at 100 volt-amps, was used to maintain a constant 118 volt supply. The voltage regulator was housed in the instrument cabinet.

The camera was mounted in a manner similar to the laser mounting, with similar allowed movements.

The Test Cell

Many different types of test cells have been designed and employed in diffusion experiments in order to establish a sharp, flat initial boundary between two fluids of only slightly varying composition. Among these are the draw slide cell, the sliding solvent cell, the flowing junction cell and the capillary withdrawal cell.

In the draw slide cell, first introduced by Lamm (39), a thin physical barrier initially separates the two fluids. When the diffusion run is initiated, the barrier is withdrawn forming the boundary. Rate of withdrawal of the barrier is critical in order that convection in the cell should be minimized.

In the sliding solvent cell, the initial boundary is formed by sliding a chamber containing one of the fluids directly over another chamber, of identical cross section,

containing the second fluid. Moving surfaces in this type cell require lubrication which often results in contamination of the test fluids. Several designs of this type of cell have been used by various investigators (9, 13, 20, 48).

In the flowing junction cell the initial boundary is formed by allowing the two fluids to flow simultaneously out of the cell through horizontal exit slits in each side of the cell at the elevation where the boundary is to be formed (9). During initial boundary formation fresh solutions flow into the top and bottom of the cell from external reservoirs. When a suitable initial boundary is formed, fluid efflux from the cell is stopped and the experiment is begun. At time zero in the experiment, when the solution efflux is stopped there is no disturbance to the system. Flowing junction cells are suitable for very high viscosities as well as for low viscosities. They have been used successfully by many investigators (12, 44, 52, 57, 59, 60).

The capillary withdrawal cell is actually a modified flowing junction cell. In this type of cell a fine capillary tube is inserted into the diffusion cell and the end of the tube is located at the level of the slits in the cell where the initial boundary is to be formed (35). Initial boundary "sharpening" is accomplished by siphoning off fluid through the capillary and the side wall slits while fresh supplies of both fluids flow into the top and bottom of the cell from external reservoirs. At time zero, fluid withdrawal

is stopped, the capillary is removed, and the experiment is begun. Considerable skill is required to properly position the capillary tube at the level of the slits in the cell walls. Much care must be exercised in removing the capillary to avoid establishing convection currents. For fluids having viscosities less than about one poise this technique has been used successfully by a number of investigators (2, 25, 26, 35, 38).

A detailed study of boundary formation in each of these cell types was performed by Bryngdahl (9). All of the types of cells gave good initial boundaries, even for very small concentration differences. However, the flowing junction cell was most advantageous since the boundary formation could be observed visually during the formation process and adjustments in rates of flow of fluids could be made as needed. Also this type of cell is most amenable to use at higher pressures since there are no moving parts which introduce sealing problems. For these reasons the flowing junction cell was selected for use in this study. The assembled diffusion cell, with the forward window removed, is shown in Figure 5, and a schematic representation is shown in Figure 6.

The test cell design was based on that of Svensson (59) and Skinner (57). The body of the cell was made of 316 stainless steel and was clad with 1-inch thick copper sheet. Dimensions of the fluid cavity in the cell were 1/4 inch wide by 3 1/2 inches high by 3 inches thick,

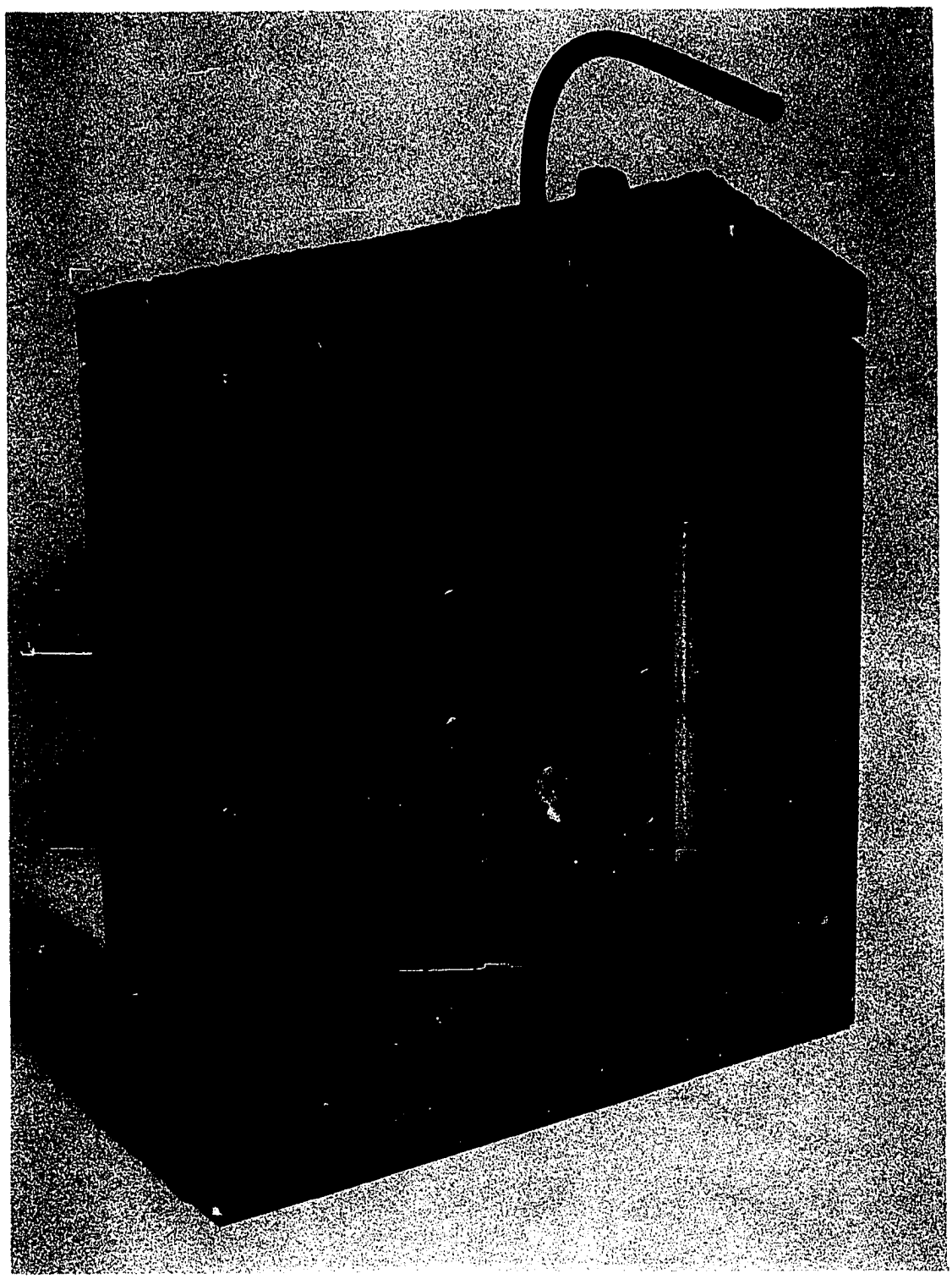

Figure 5. Photograph of Assembled Diffusion Test Cell

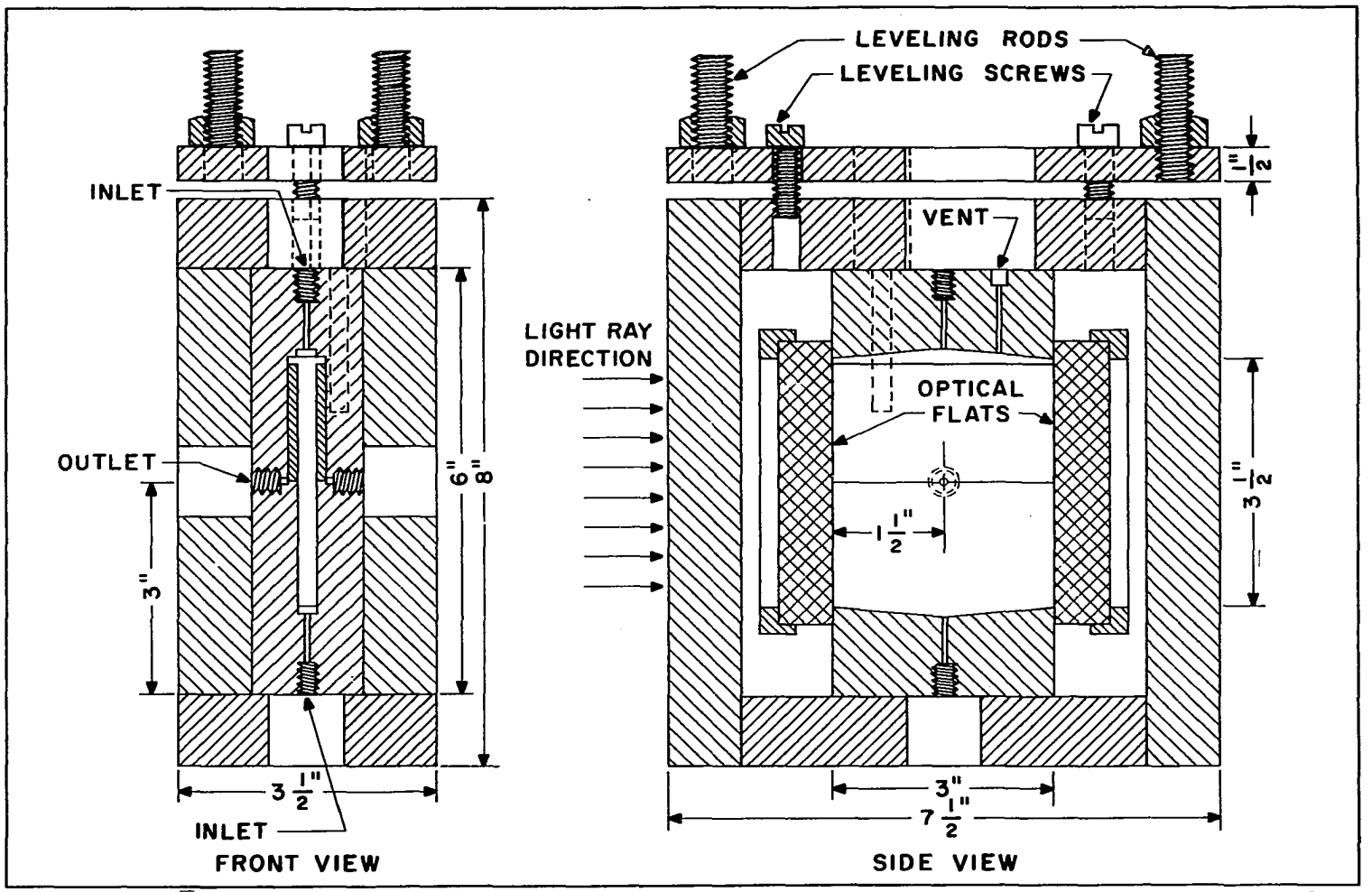

Figure 6. Schematic Drawing of the Diffusion Test Cell

giving a geometrical light path through the cell of three inches. Cell windows, which were mounted on rubber gaskets 1/32 inch thick on each cell face, were held in adjustable brackets which allowed setting the windows normal to the entering collimated light beam. Each cell window was 3/4 inch thick by 1 inch wide by 4 inches long. They were made of Schott BK-7 optical glass polished flat to 1000 Å or less with surfaces parallel to 15 seconds or less.

The upper sidewall sections of the cell cavity, above the slit, were removable plates to allow adjustment in the cell slit width. For the studies performed here the slit width was set at 0.0015 inches and the plates were cemented into the cell using General Electric Silicone Rubber Cement RTV-108, which was unaffected by the fluids used. On both sides of the cell, the back side of the slit was beveled on a 45° angle over one-fourth of the depth of the slit to form a manifold for draining the fluid through the slit. This gave a more uniform initial boundary than could be obtained without such a manifold. Behind the slits in the center of the side walls of the cell, holes were drilled and tapped for 5/16 inch 24 thread per inch special O-ring seal fittings, with 1/8 inch compression tubing connections on the opposite end of the fittings. The final 1/8 inch of wall thickness was drilled into the slit using a 1/32 inch drill bit. The top and bottom of the cell were similarly prepared. In addition a 1/4 inch stainless steel vent tube was silver soldered into the top of the cell adjacent to the cell inlet.

A 1/4 inch diameter hole, two inches in depth, was bored into the top of the cell in the side wall for insertion of a platinum resistance thermometer capsule. However, for these experiments all temperature measurements were made using copper-constantan thermocouples.

Inlets to the cell were connected to fluid reservoirs by 1/8 inch stainless steel tubing. The fluid reservoirs were constructed of 3 inch diameter 316 stainless steel pipe and 316 stainless steel plate. The top of each reservoir was threaded and equipped with an O-ring seal. One of the fluid holding reservoirs is shown in Figure 7.

The cell outlets at the side wall slits were manifolded with 1/8 inch stainless steel tubing and connected to a drain. In each of the inlet lines and the drain line, an electrical pulse-operated latching valve (Skinner Electric Valve Co., New Britain, Conn.) and a 1/8 inch Whitey needle valve were installed. Adjustments of the relative flow rates of the fluids and the overall flow rate were made using the needle valves, while the latching valves gave a quick and positive shutoff at the beginning of each diffusion run. The latching valves operated on 24 volt DC electrical power. A 20 millisecond pulse in one direction opened the valve and latched it open. When the polarity was reversed a 20 millisecond pulse closed the valve and latched it in a closed position. All of the tubing fittings used in the system were Swagelock 1/8 inch 316 stainless

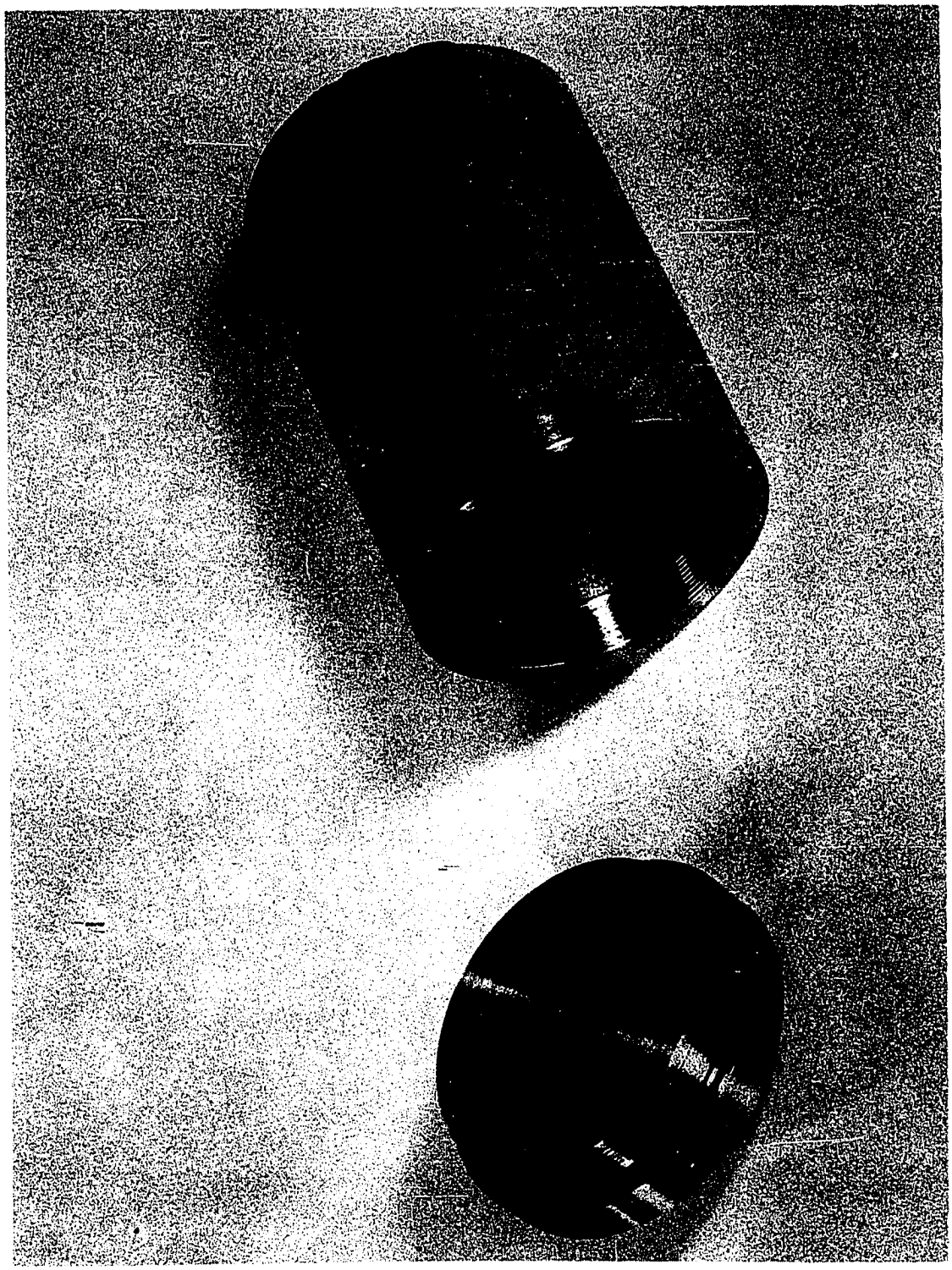

Figure 7. Photograph of Fluid Holding Reservoir

steel compression fittings (Crawford Fitting Co., Cleveland, Ohio).

Teflon tape was used on all thread connections on the cell, fluid holding vessels and valves. Use of the teflon tape improved the seal around the threads and also prevented galling of the stainless threads. Stem extensions were made for all valves so that the valves could be operated from outside the constant temperature air bath.

The cell and fluid holding reservoirs with integral tubing connections and valves were mounted on a bracket so they could be removed from the air bath as a unit. Cell removal was accomplished by merely unbolting the bracket, disconnecting the vent line, drain line, valve stem extensions, and disconnecting the electrical leads to the latching valves. The cell and fluid reservoirs were mounted on the bracket in such a manner that adjustments in their elevation and level could be made in aligning the system. Devices attached to the bracket allowed both horizontal and longitudinal adjustment of the bracket to align the cell in the optical path.

The bracket was bolted to an adjustable mount connected to the optical bench. Cross members of the mount passed through the walls of the constant temperature air bath with all parts of the mount being insulated from the bath with soft rubber gaskets. Valve stem extensions also passed through the walls of the bath and were similarly insulated from the bath. In this manner any vibration emanating from the bath was minimized before reaching the cell.

The Constant Temperature Air Bath

The constant temperature air bath was mounted on a separate frame which also served as the housing for the temperature control instruments. The air bath consisted of a double wall box with a 3 1/2-inch thick annular space that was filled with perlite for insulation; box walls were constructed of 3/4-inch plywood on a metal frame. A removable top was constructed for the bath.

Inside dimensions of the air bath were 16 inches along the optical bench by 22 inches wide by 22 inches deep. Plexiglass baffles 1/4 inch thick were spaced 3 inches in from each side wall of the bath, parallel to the optical bench. The baffles were set 2 1/2 inches above the bottom of the bath with a 2 1/2 inch overflow space at the top of the bath.

For the bath windows in the optical path, special window mounts were constructed which consisted of flanges affixed to the ends of a 4-inch I.D. stainless steel tube. The flanges were of two-piece construction, one piece affixed to the stainless tube with set screws and also fixed to the wall of the air bath with threaded rod, and the other was slotted and recessed to hold a 4 1/2-inch diameter window, 3/4 inches thick. The flange part affixed to the stainless tube was slightly oversized to allow for some leveling adjustment with the set screws. Bath windows were also made of Schott BK-7 optical glass polished to the same specifications as the cell windows. Silicone

rubber O-rings resting in grooves machined in each end of the 4-inch I.D. tube gave a seal between the windows and tubing and also allowed some degree of adjustment in the windows. A vacuum was maintained in the tubing between the two windows as a means of preventing condensation on the inner window surfaces. Air-spaced plate glass viewing windows were installed on the other side walls of the cabinet. The internal portion of the air bath was equipped with heater elements, baffles, an air circulating fan and temperature sensing elements. Figure 8 is a schematic representation of the air bath with the cell and fluid reservoirs in place.

The air circulating fan was installed on a shaft through two high speed bearings mounted on the bottom of the air bath, one inside and one outside of the bath. A pulley was attached to the lower end of the shaft outside of the bath and the fan was belt driven by a 1/4 horsepower, 110 volt AC Dayton split phase motor. Speed of fan rotation was altered by interchanging pulleys on the fan shaft and motor shaft. A four wing fan blade was used. It was a 14 inch diameter heavy duty blade with 32° pitch, and was mounted on a 3/8 inch diameter shaft. At 1500 rpm the rated delivery for this blade in open air was 1480 cubic feet per minute with a 1/25 horsepower expenditure. Through experimentation it was found that best temperature control was attained when the fan speed was maintained at about 750 rpm. No measurements were made of the actual air flow rate through the bath.

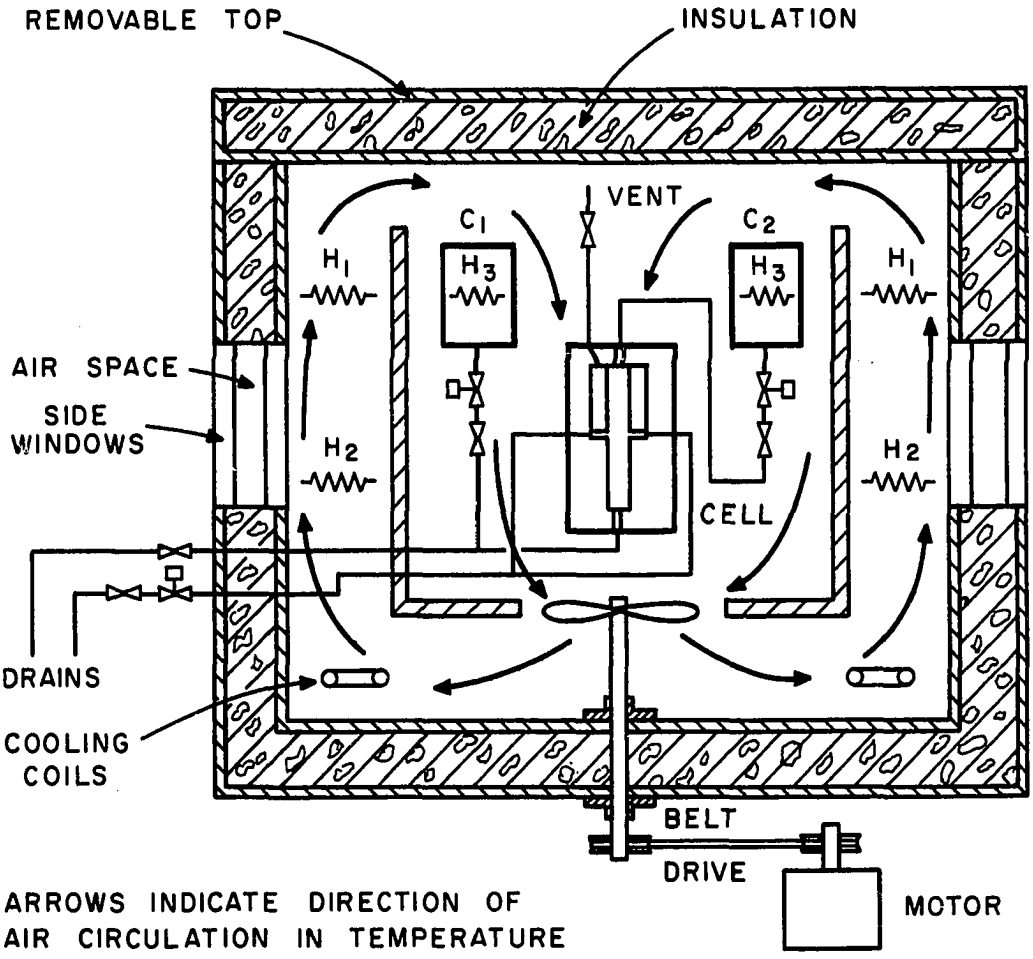

NEEDLE VALVE

SOLENOID VALVE

H_1 CONTROL HEATER, CONNECTED TO CONTROL SYSTEM

H_2 AUXILIARY HEATER, CONNECTED TO STABLE POWER SUPPLY

H_3 QUICK HEATER FOR FLUID VESSEL, CONNECTED TO STABLE BUT VARIABLE POWER SUPPLY

Figure 8. Schematic Diagram of Constant Temperature Air Bath

The fan circulated the air over the heating elements, around the baffles and through the central portion of the bath where the cell was mounted. Temperatures in the fluid reservoirs, the cell and the air space at the top and bottom of the bath were measured with copper-constantan thermocouples using an 8686 Millivolt Potentiometer (Leeds and Northrup). Bath temperature was sensed with unshielded nickel wound resistance elements. Signals from the nickel wound elements were fed to a temperature controller (Hallikainen Thermotrol, Serial Number 14872) and a differential temperature recording device (Hallikainen Thermograph, Serial Number 13058). The temperature controller operated a heater element which was continuously adjustable from 0 to 280 watts. An auxiliary heating element, continuously adjustable from 0 to 660 watts supplied the bulk of power required to overcome heat losses while the smaller heater was used as a control medium.

For experimental work at or below room temperature, the constant temperature bath was equipped with cooling coils for the circulation of either chilled water or Freon refrigerant.

It was found that the temperature of the fluid reservoirs lagged the cell temperature significantly, during the period the bath was being brought up to the temperature of the experiments. To assist in heating the reservoirs to near control temperature, an individually operated 40 ohm immersion heater was inserted into each reservoir.

AC power at 32 volts was supplied to these heaters through an oil sealed line transformer. This reduced the time required to heat the bath from room temperature to steady state temperatures of approximately 65°C, from near 14 hours to about 4 hours.

A number of temperature control experiments were performed covering the range from room temperature to 80°C. Over this range, the temperature at the position of the nickel wound elements could be controlled to within 0.01°C. At steady state no temperature gradients in the bath could be detected with the thermocouples located throughout the system. Schematic diagrams of the electrical circuits of the control system are shown in Figures 9 and 10. All of the control system elements, with the exception of the Thermotrol, Thermograph and Millivolt Potentiometer were panel mounted. The control panel can be seen in Figure 1.

Time Measurement System

Time measurements for the experiments were made using a precision tenth second elapsed time electric timer (Precision Timer Co., Inc.). Range of the timer was from 0 to 9999.9 seconds, and it was equipped with manual reset. Power requirement for the timer was 110 volt, 60 cycle AC. The timer was mounted in a remote control box which in turn was mounted on the optical bench adjacent to the camera. The remote control box also housed a remote switch for opening and closing the latching valves

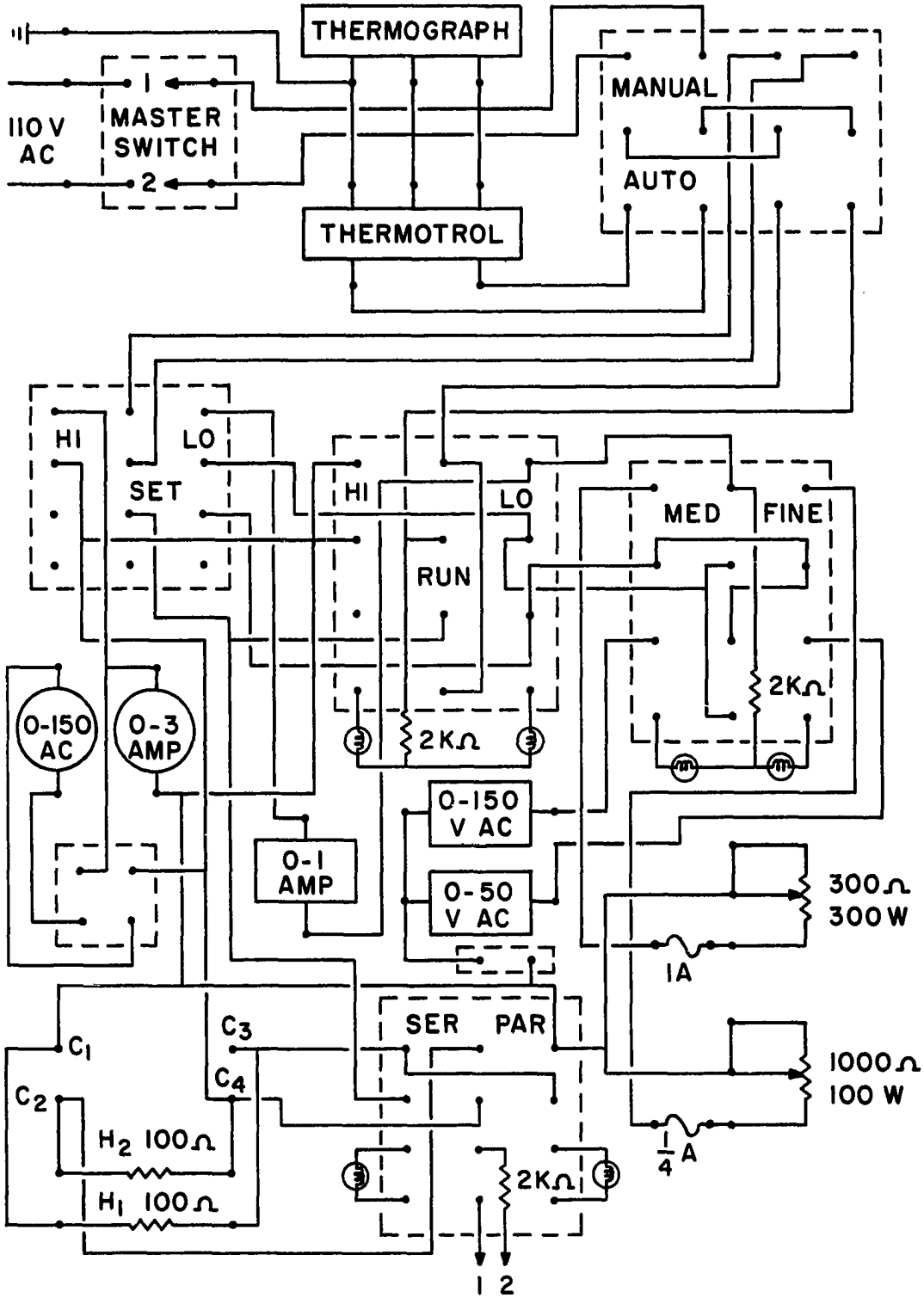

Figure 9. Wiring Diagram of the Control Heater Circuit

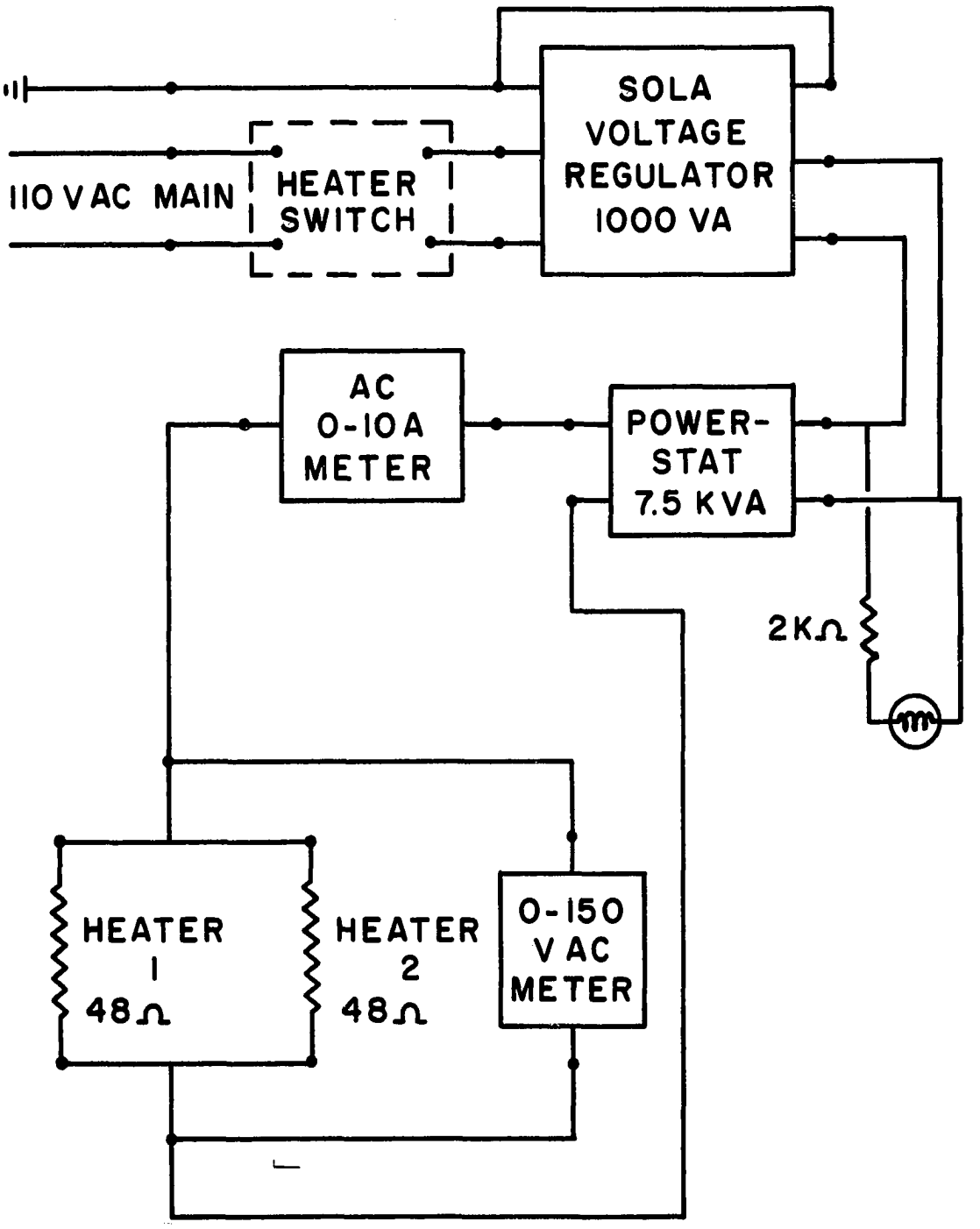

Figure 10. Wiring Diagram of the Auxiliary Heater Circuit

which isolate the cell from the drains and the fluid reservoirs. Using this arrangement it was possible to close the valves and start the time clock simultaneously at the start of a diffusion experiment. A second timer (The R. W. Cramer Co., Inc.), mounted in the remote control box as a check on the primary timing device, operated on 28 volts DC electrical power.

The power switch in the remote control box, for operating the latching valves, either opened or closed all three of the valves simultaneously. Additional switches were located on the control panel to open and close the latching valves individually.

Procedures

System Alignment

One of the major problems encountered in using interferometers in performing diffusion experiments is aligning the optical system and aligning the diffusion cell in the optical path of the interferometer. This is especially critical when using the birefringent interferometer. Following is a description of the procedure used to attain alignment of the system.

Employing a 48 inch mason's level the optical bench was leveled, both longitudinally and horizontally, and locked into place using the integral bolts on the concrete mounting pilars.

Prior to filling the annular space of the constant temperature bath with perlite insulation, the window mounts were installed in the bath. The flange parts affixed to each of the ends of the stainless tubing were bolted together through the walls of the bath and the tubing sections were simultaneously leveled and evened using a sensitive 28 inch carpenter's level and the set screws on the flange pieces. Centers of the stainless tubing were then aligned with the centerline of the optical bench. Again the level of the tubing was checked and minor adjustments were made as needed.

Thin circular discs, the size of the windows for the constant temperature bath and of each lens in the system, were made from black art paper. Squares, 1 1/2 inches on a side, were made to represent the Savart plates but were further treated in the same manner as were the discs. A pinhole, approximately .01 inches diameter, was located in the geometric center of each disc. Each pinhole was cut with a leather punch to yield a smooth hole and thus minimize refraction around the edges of the hole.

The discs the size of the constant temperature bath windows were centered on and affixed to the ends of the stainless tubing on both sides of the bath. The laser was positioned and bolted down to its mount. Using the collimated beam of the laser as an aligning tool, the laser mount was adjusted until the laser beam striking the pinhole in the disc in the window nearest the laser was in

perfect alignment with the pinhole in the disc in the second window mount.

At this point the level of the beam was checked using a cathetometer with a telescope and Gauss eyepiece (Gaertner Scientific Corporation, Chicago, Illinois) which was located on the centerline of the optical bench at the opposite end of the system from the laser. Again minor adjustments were made in the positioning of the constant temperature bath and the laser until the alignment of the laser beam through the pinholes of the discs on the window mounts and into the Gauss eyepiece was as nearly perfect as possible.

Focal lengths of the lenses used in the system were determined to within plus or minus a half inch. The lens mounts for the various lenses, affixed to magnesium plates, were positioned on the optical bench, according to the lens focal length. They were then leveled on pipe stanchions and affixed to the optical bench with 1/2 inch threaded steel rod.

The discs, the size of each lens, were centered in the lens holder of each lens mount in turn, beginning with the mount nearest the laser. Each lens mount was adjusted, using the various movements built into the mount, until the laser Beam was exactly centered on the pinhole in the disc. At each step the level and alignment of the laser beam through the pinholes and into the Gauss eyepiece were checked.

This procedure was continued until the geometric center of each lens holder and the window mounts of the constant temperature bath were aligned. At this point all of the discs were removed from the optical system.

One by one the windows of the temperature bath were installed in their mounts. Each window was adjusted until it was precisely normal to the laser beam. This was accomplished by adjusting the window until the reflections returned to precisely their point of origin on the front mirror of the laser.

Even though the distance from the window nearest the cathetometer and Gauss eyepiece was approximately 15 feet, no refraction of the laser beam could be observed after mounting the four windows on the constant temperature bath. This indicated that the composite parallelism in the four windows, randomly mounted, was well within the tolerance specified for each of the windows when purchased. For example, 15 seconds deviation in window parallelism over a 15 foot distance would cause a refraction of approximately 1/64 inch, which would be large enough to be observed in the Gauss eyepiece.

The Savart plates were then positioned in their holders and adjusted normal to the laser beam employing the same reflection technique which was used on the windows of the constant temperature bath.

Mounting of the lenses was the next step. It can be seen by referring to Figure 3 that the laser beam is

alternately focused and recollimated by each pair of lenses in order, beginning with L_1 nearest the laser. Further alignment takes advantage of this fact. For perfect lenses the perfection in collimation of a light beam is determined by the exactness attained in matching the focal points of the lenses.

Each pair of lenses was mounted in order, beginning with L_1 and L_2 nearest the laser. L_1 was a converging lens 18.3 mm in diameter with a focal length of 39 mm. By means of this lens the collimated beam of the laser was expanded to a four inch diameter at L_2. The two lenses L_2 were a matched pair, 4 1/8 inches in diameter with a 60 inch focal length, and were air-spaced achromatic lenses. The 4 inch beam was recollimated by L_2 nearest the laser.

To match the focal points of L_1 and L_2 a screen was made of black art paper. A pinhole, approximately .01 inch, was made in the center of the screen. With the laser beam passing through L_1, the pinhole in the screen was positioned at the focal point of L_1 so that L_2 was illuminated. Using a first surface mirror on the side of L_2 farthest from the laser, the laser beam was reflected back through L_2 at a very small angle such that the reflected light struck the screen. The lens mount for L_1 and the screen were then moved longitudinally along the optical path until the focal point of L_2 was found on the screen. This matches the focal points of the two lenses.

Ordinarily the light beam was reflected back through L_2 so that its focal point on the screen was within one half inch of the pinhole. This distance was maintained small to minimize any imperfections in locating the screen perfectly normal to the centerline of the laser beam.

The above procedure was employed between the lens L_2 farthest from the laser and L_3. L_3 had a diameter of 35 mm and a focal length of 180 mm. Lens L_4 had a diameter of 35 mm and a focal length of 200 mm. It was adjusted longitudinally until its focal point was located at a point approximately 1 inch behind the second Savart plate, S_2. The collimation of the laser beam between L_3 and L_4 through the first Savart plate, S_1, was tested using a screen to determine variations in image size between the two lenses. If any such variations existed they were too small to be detected.

After the focal points were matched the lenses were removed from the mounts; the discs were relocated in the mounts and centerline alignment was again checked to determine if the longitudinal movement of the mounts had affected the alignment. No detectable change could be noted. The clamps and locking screws on the lense mounts were then set to lock the mounts into position. The lenses were cleaned and replaced in their respective mounts.

The Savart plates, S_1 and S_2, were replaced in their mounts. Rotation adjustments were made in S_2 until the interference patterns obtained in passing the laser beam

through the constant temperature bath, with no temperature or concentration gradients, were determined to be vertical by employing a plumb bob. Then the rotation adjustment of S_2 was locked into position. Further rotation adjustment of S_1 could only be made during a trial diffusion experiment. This adjustment did not affect the previous adjustment of S_2; therefore it will be discussed later.

Cell Alignment

The procedure for alignment of the diffusion cell was actually performed as two separate stages. The first stage was done during alignment of the optical system and the second stage was done after all other optical components were in place.

To align the cell it was necessary to make adjustments so that the slits in the side walls of the cell were level and parallel to the center line of the laser beam passing through the constant temperature bath. It was necessary that the windows on the cell be normal to the laser beam. For the first stage of cell alignment the cell windows were removed.

After the mounts for the optical components of the system were aligned and centered, the cell and fluid reservoirs mounted on the bracket were inserted into the bath. A stainless steel 0.0015 inch thick spacing gage, which had been machined to the proper width, was inserted into the cell slits. The gage was sufficiently wide to just traverse

the width of the cell and slits with no strain on the gage. This allowed the gage to lie in a flat position across the cell in both longitudinal and horizontal directions.

With the collimated beam of the laser passing through the constant temperature bath, the cell was adjusted vertically, using the leveling rods on the cell shown in Figure 6, until the laser beam was split above and below the thickness gage. The thickness gage was polished to make the surface give maximum reflections. When the cell was level the reflections from the gage surface were minimal and the size of the laser beam at the end of the optical bench opposite the laser was also minimal on a screen located at that point. The fine leveling adjustment of the cell was accomplished using the leveling screws on the cell.

When the cell was level in the constant temperature bath the vertical adjusting mechanisms of the assembly were locked into place. By removing the cell and reinserting it into the constant temperature bath a large number of times, it was found that the vertical adjustment of the cell was unaffected.

The horizontal adjustment of the cell was accomplished in much the same manner. However, the horizontal adjustment was performed after the windows of the constant temperature bath, the lens L_1 and the lens L_2 nearest the laser were all fully adjusted in the optical system.

Since the vertical walls on the interior of the cell were also highly polished, the proper horizontal position

of the cell was stable on the mount and the cell could be properly positioned both vertically and horizontally by returning it to the constant temperature bath at the marked position.

To adjust the cell windows, the cell was removed from the constant temperature bath, and one of the cell windows, its gasket and window bracket were positioned on the cell. The cell was returned to the bath and positioned. The window was adjusted normal to the laser beam by adjusting the window set screws until the light reflections from the surfaces of the windows returned exactly to their point or origin on the front mirror of the laser, as was done for each of the windows of the constant temperature bath. The cell was again removed from the bath and the other window, gasket and window bracket were positioned on the cell. Then the cell was again positioned in the bath and the second window was adjusted normal to the laser beam in the same manner as was the first window.

After the windows were adjusted, the cell was tested and was found to be free from leaks. Adjustments of the cell windows were made in the same way each time the cell was removed from the constant temperature bath for cleaning.

Periodically, during the experimental work, the alignment of the entire system was checked to assure alignment stability.

Diffusion Experiments

The procedure followed in setting up and performing a diffusion experiment was originally less explicit than any other procedure. However, as more experience was gained in using the equipment, a more firm procedure was established.

In the early diffusion runs the diffusion cell and integral components were inserted into the constant temperature bath and positioned. Final adjustment was made on the cell windows as per the above cell alignment procedure. The bracket, on which the cell and fluid reservoirs were mounted, was bolted into position. The vent line drain lines, electrical leads to the latching valves and the valve stem extensions were connected. Thermocouples were positioned in the cell, fluid reservoirs and the constant temperature bath. The vent line valve was opened and all other valves were closed. The fluid reservoir, which fed fluid to the bottom of the cell, was filled with the more dense of the two fluids to be used in the experiment.

The flow valve to this reservoir was then opened and the cell and all flow lines were filled with the more dense fluid. In order to totally fill the cell a vacuum was pulled on the cell vent line. When the cell was completely filled, the vent line valve was closed and the drain line valves were opened. About 200 milliliters of the more dense fluid were allowed to flow into the cell and out the cell slits to displace the last traces of air in the cell system. Then all valves were closed.

Both fluid reservoirs were then filled with the proper fluids and the auxiliary heaters for the fluid reservoirs were inserted into the fluid reservoirs. The lid of the constant temperature bath was installed and bolted into position, and the fan was started. Power to the auxiliary bath heater was turned on, and the control rheostat for the auxiliary bath heater was set at the desired level. To start the operation of the control heater, the Thermotrol was set for the desired control temperature. The rheostat on the control heater was adjusted for maximum power to the control heater. To trace the temperature-time curve of the heat-up period the Thermograph was used. Chart speed was set at 4 inches per hour and full scale deflection of the recorder was set sufficiently high to cover the full range of temperature rise during heat-up.

Temperatures in the constant temperature bath, in the cell and in the fluid reservoirs were measured periodically as the bath heated up. Also the auxiliary heaters in the fluid reservoirs were turned on periodically for short intervals to minimize the temperature lag between the fluid reservoirs and the bath. During these periods the temperatures of the fluid reservoirs were closely monitored.

When the Thermotrol began to function on control, the power input to the control heater was slowly reduced until the ratio of off time to on time of the control heater was approximately four. This was the optimum ratio

specified for the controller by the manufacturer. The full scale range of the Thermograph was slowly reduced until, at even control, full scale deflection was only 0.2°C. After no difference in temperature could be determined on any of the thermocouples in the bath, fluid reservoirs and the cell, the temperature in the constant temperature bath was allowed to equilibrate for an hour longer. Figure 11 shows the recorded deviation in temperature at the point of the open nickel wound sensing element in the constant temperature bath during experimental run No. A-TEG-17 where the absolute control temperature was 30 ± 0.1°C. Some difficulty was experienced in exactly reproducing the set temperature for the various experiments but with experience the control point could be set to within ±0.1°C.

After temperature equilibrium was established in the system the valves on the fluid reservoirs and on the drain through the cell slits were opened to begin establishing the initial boundary in the cell. Effluent rate to the drain was set at about 10 to 12 drops per minute. After about 30 minutes, or when an initial boundary could be seen in the cell with the naked eye, the laser was turned on.

Boundary sharpening was then followed visually through the lens of the camera. Focusing of the camera will be described later. The relative rates of flow of the two fluids were manipulated by adjustment of the needle valves on the lines to the fluid reservoirs to obtain the

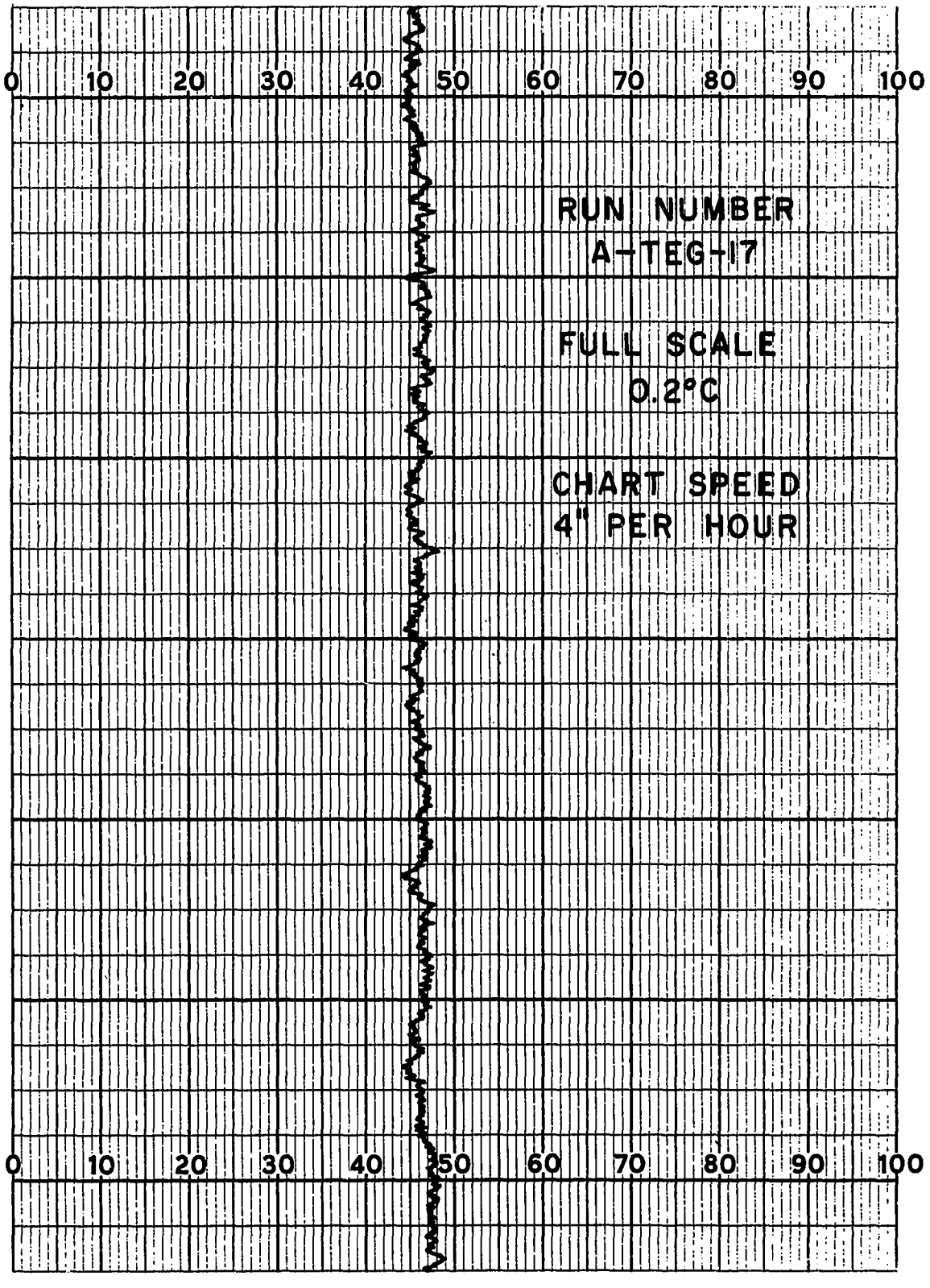

Figure 11. Deviation of Temperature from the Set Point During Experimental Run Number A-TEG-17

sharpest possible initial boundary. Formation of the desired initial boundary was quite delicate and often required numerous small adjustments in the relative rates of flow of the two fluids. This was done mostly by trial and error procedure.

During this time the camera was loaded with film in preparation for the start of the diffusion run. Usually about 250 to 350 milliliters of each of the fluids had to be flowed through the cell to form the initial boundary.

When the initial boundary was as sharp as could be obtained, the latching valves were closed and the time clocks were activated simultaneously. An exposure of the interference pattern was made every 25 seconds in the early history of the run for about the first 300 seconds. In the further history of the run exposures were made every 50 to 250 seconds depending upon the visual observation of the rate of movement of the interference pattern. The faster the apparent movement of the interference pattern, the shorter was the time interval between exposures.

In all, at least 36 exposures were made on each diffusion run. The length of the runs varied from about 2500 seconds to about 15,000 seconds.

In the early experiments the fluid viscosities were in the range from about 0.6 to about 3 centipoises. For this range of viscosities the above prescribed procedure was found to be highly satisfactory. However, when fluids having higher viscosities were used, the original loading of the cell had to be altered.

With the higher viscosity fluids it was found that the displacement of the more dense fluid by the less dense fluid was not highly efficient. That is to say, the fluid along and near the cell walls was displaced so slowly from the top of the cell that fluid volumes in excess of the volumes of the fluid reservoirs would be required to establish a suitable initial boundary.

Therefore, when the viscosities of the fluids used were in excess of about 3 to 4 centipoise, the cell was only filled to the slit level with the more dense fluid on the original filling step. The drain lines were also filled with the more dense fluid. Then as before all valves were closed; both fluid reservoirs were filled and the auxiliary heaters for the fluid reservoirs were inserted into the fluid reservoirs. The top of the constant temperature bath was positioned and bolted into place, and the heating-up period was begun.

When temperature equilibrium was attained, a moderate vacuum was pulled on the cell with the vent line open. The valve was opened on the fluid reservoir containing the least dense of the two fluids used in the test to allow it to enter and fill the remainder of the cell volume. This filling procedure was found to be satisfactory and allowed a suitable initial boundary to be formed by flowing only 400 to 500 milliliters of the fluids into the cell while drawing off fluid through the cell slits. However, for the higher viscosity fluids the draw-off rate had to be

reduced to about 8 to 10 drops per minute to obtain a suitable initial boundary.

To accomplish the latter filling procedure, a connection to the vent line had to be installed through the wall of the constant temperature bath for pulling the vacuum on the cell. As in the case of the drain lines and the valve stem extensions, the connection to the vent line was installed through soft rubber gaskets on both the inside and outside walls of the bath.

Since this optical method employed very small density differences between the more dense and least dense fluids, a high degree of temperature control was mandatory. In some of the testing it was found that for density differences on the order of 0.1% between the two fluids that an $0.5^{\circ}F$ temperature difference between the two fluids could cause a density inversion.

Adjustment of Savart Plate S_1

Adjustment of Savart plate S_1 in the optical system was critical. To accomplish its exact adjustment, it was necessary to perform a preliminary experiment.

In this experiment performed at room temperature of $23^{\circ}C.$, an 0.1 weight percent aqueous solution of sucrose was used. An initial boundary condition that could be observed with the naked eye was established between this solution and distilled water. The diffusion run was

started and allowed to proceed for about 3000 seconds. A polarizer and ground glass screen were placed in that order between Savart plate S_1 and lens L_4. With the proper adjustment at this point the interference pattern should be a series of horizontal interference fringes. S_1 was rotated in its holder until the horizontal fringe pattern was observed. The experiment was allowed to continue for an additional 5000 seconds. During this time, as the fringes moved out from the center of the cell, the adjustment of S_1 was checked on 500 second intervals to ascertain that no bending of the interference fringes occurred. No additional adjustments had to be made for the S_1 rotation position. Savart plate S_1 was then locked into position.

Camera Focusing

Considerable difficulty was experienced in finding the proper location for mounting the camera. At first the camera was mounted on a tripod so that its proper location could be found by moving the camera toward and away from Savart plate S_2 on the optical axis of the system. This had to be done during a diffusion run. So again an 0.1 weight percent aqueous solution of sucrose was used for this purpose.

During the location of the proper camera position it was found that a large magnification of the image was necessary to obtain photographs sufficiently large to

observe the interference patterns. The required magnification was obtained by use of a bellows attachment and a set of ring extenders. When the approximate location of the camera was found the camera mount was constructed and affixed to the optical bench. The camera was bolted to its mount and the fine focusing was then accomplished.

To eliminate the aberration corresponding to Weiner skewness of the gradient curve, which is represented by the interference pattern observed through the camera, the experiment was allowed to progress sufficiently long that the entire interference pattern showed up in the image. Then the camera was adjusted until the skewness was eliminated. This corresponds to focusing the camera on a plane 1/3 of the distance through the diffusion test cell, measured from the cell face nearest the laser (61, 62).

Selection of Photographic Film

Since the wave length of the laser beam (6328Å) was in the red light region it was necessary to select a film which gave the proper sensitivity. Panchromatic films satisfied this requirement.

To select the proper film exposure and the most suitable type of panchromatic film (Pan-X, Plus-X, or Tri-X) a series of preliminary diffusion experiments was performed. Interference patterns were recorded at various exposures using the three film types. It was found that the fine grain of Pan-X film made this film most suitable for recording the data.

In the early history of the experiments, when the interference patterns were sharpest, exposures of 1/15 second gave superior recordings. In the later history of the experiment it was found that increasing exposure time to 1/8 second and, then, at later times to 1/4 second and 1/2 second gave the most distinct recordings.

After completing these preliminary tests, it was found that changing the exposure time to obtain the best recording of the data during individual runs became a matter of experience. Due to improper setting of exposure time, a number of the early experimental runs could not be interpreted because the incerference patterns were too indistinct.

Interpretation of Data

The concentration difference between the more dense and less dense triethylene glycol-water solutions was held to one weight percent or less. Under this condition it was assumed that Fick's second law, equation (24), held and that the diffusion coefficient was constant over this range of concentrations.

With an infinitely sharp initial boundary between the two solutions in the diffusion cell, a constant diffusion coefficient, and with a sufficiently long diffusion path above and below the initial boundary the solution to equation (24) becomes

$$\frac{C_A(\xi,t)-C_{A0}}{C_{A1}-C_{A0}} = 1/2 \left\{1 + \text{erf} \frac{\xi}{\sqrt{4D_{AB}t}}\right\} \qquad (46)$$

for one dimensional diffusion. Equation (46) relates the concentration of component A for a binary solution at point ξ and time t to the original concentrations of the two solutions and the diffusion coefficient. $\text{erf} \frac{\xi}{\sqrt{4D_{AB}t}}$ is defined as

$$\text{erf} \frac{\xi}{\sqrt{4D_{AB}t}} = \frac{2}{\sqrt{\pi}} \int_0^{\frac{\xi}{\sqrt{4D_{AB}t}}} e^{-z^2} dz \quad . \qquad (47)$$

Over small concentration intervals, the refractive index of the solutions was considered to vary linearly with concentration. The product of the refractive index, n, and the geometrical length, α, through the test cell is defined as the length of the optical path, Z, and is given by

$$Z(\xi,t) = \alpha n(\xi,t) = \alpha[k_0 + k_1\{C_A(\xi,t)-C_{A0}\}]. \qquad (48)$$

Solving equation (48) explicitly for $C_A(\xi,t)$ results in

$$C_A(\xi,t) = \frac{Z(\xi,t)}{k_1\alpha} - \frac{k_0}{k_1} + C_{A0} \qquad (49)$$

which when substituted into equation (46) yields

$$\frac{Z(\xi,t)-Z_o}{Z_1-Z_o} = 1/2 \left\{1+\text{erf} \frac{\xi}{\sqrt{4D_{AB}t}}\right\} \quad . \qquad (50)$$

The interference pattern provided by the birefringent interferometer was an optical path gradient. This gradient was recorded on film at various constant times, t_i. For this condition, differentiating equation (50) holding time constant yields

$$\left\{\frac{\partial Z(\xi,t)}{\partial \xi}\right\}_t = \frac{Z_1-Z_o}{2\sqrt{\pi D_{AB}t}} \exp\left\{-\frac{\xi^2}{4D_{AB}t}\right\} . \qquad (51)$$

For two times t_i and t_j, at constant values of the optical path gradient, equation (51) may be solved for D_{AB} to obtain

$$D_{AB} = \frac{\frac{(2\xi_i)^2}{t_i} - \frac{(2\xi_j)^2}{t_j}}{8 \ln \frac{t_j}{t_i}} \qquad (52)$$

where ξ_i and ξ_j refer to the cell coordinates at which the gradient is measured at t_i and t_j respectively.

Through the use of equation (52) and photographic recordings of the optical path gradient at a number of different times, following the initiation of the experiment, the diffusion coefficient was determined.

It was not possible to establish an infinitely sharp initial boundary. However, it has been shown (18, 43)

that the initial condition can be properly corrected mathematically. This involves determination of a zero time correction, Δt, to account for the imperfection in the initial boundary between the two solutions. Since the exact method used in the present study had not been used previously it was necessary to derive an expression for the zero time correction. Using the derived time correction, the final expression for the diffusion coefficient became

$$D_{AB} = \frac{D'_{AB}}{(1+\Delta t'\theta)} \tag{53}$$

where

$$D'_{AB} = \frac{\frac{(2\xi_i)^2}{t'_i} - \frac{(2\xi_j)^2}{t'_j}}{8 \ln \frac{t'_j}{t'_i}} \tag{54}$$

and

$$\theta = \frac{t'_i+t'_j}{t'_i t'_j} - \frac{\frac{1}{t'_i} - \frac{1}{t'_j}}{\ln \frac{t'_j}{t'_i}} \quad . \tag{55}$$

By plotting D'_{AB} against θ and extrapolating the resultant straight line to $\theta=0$, i.e. t'_i and $t'_j \rightarrow \infty$, the diffusion coefficient D_{AB} is determined. The slope of the line determines the value of $\Delta t'$.

Figures 12 through 16 in Appendix C are plots of D'_{AB} against θ for the experiments performed in this study for which values of D_{AB} are reported in Tables I and II.

Derivations of equations (53)(54) and (55) are presented in Appendix B.

Measurement of Recorded Data

The films for the diffusion experiments were developed in fine grain developer and printed on proof sheets. Each print was tested for clarity of the interference pattern using a 60X precision magnifier. Enlargements, approximately three times actual size, were made from those negatives for which the prints indicated sufficiently distinct interference patterns.

Usually 15 to 20 such enlargements were made on each experimental run. A distinct image of the width of the cell cavity (actual size 1/4 inch ± 0.001 inch) was recorded on each photograph from which the actual magnification was determined. Each enlargement made from the film was focused individually, during printing, so that often the magnification factor varied from photograph to photograph.

The camera was focused such that there was no skewness in the recordings of the interference patterns. Therefore the following procedure was used to measure the recorded data. Figure 17, a mathematically derived normal distribution curve, is used here to clarify the measurement procedure.

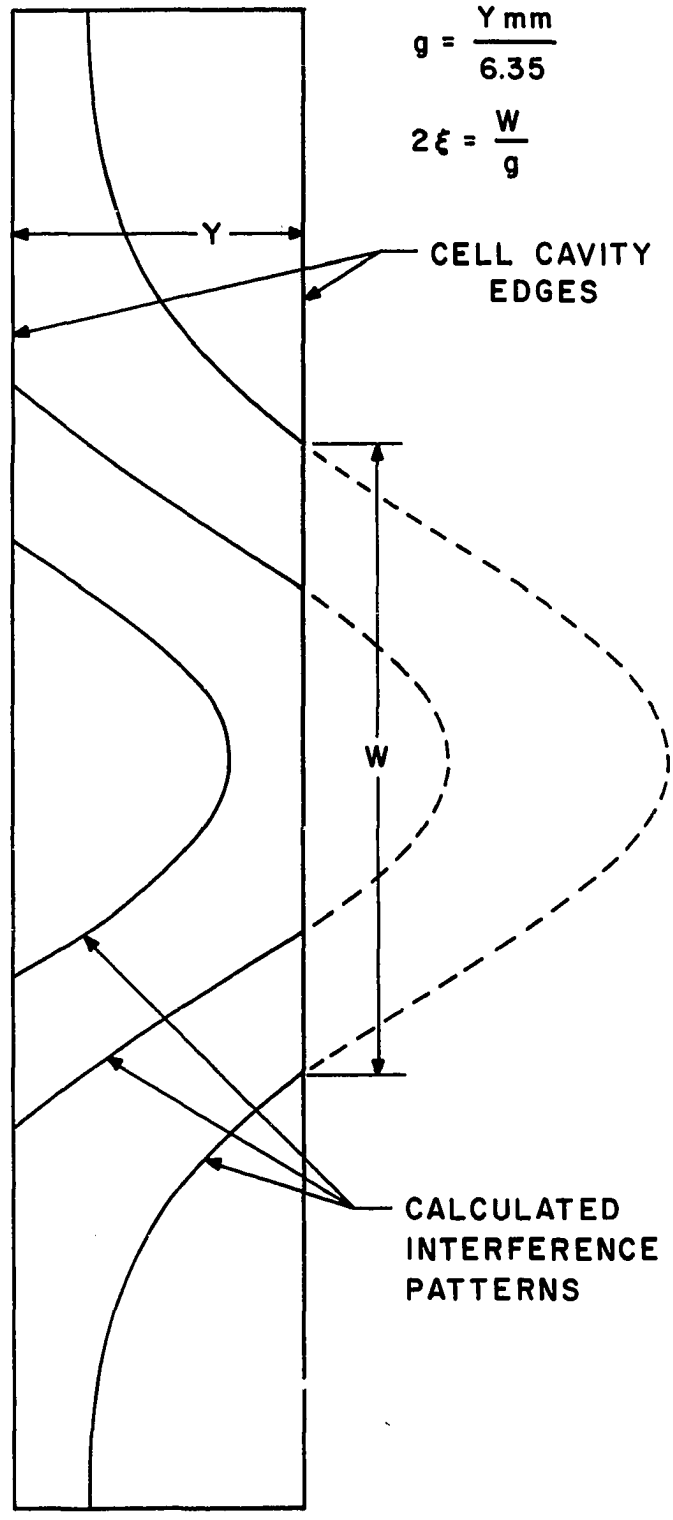

Figure 17. Mathematical Representation of Interference Pattern Showing Measurements Made on Actual Patterns

(1) Base lines were drawn along both edges of the image of the width of the cell cavity with a sharp needle. Due to magnification of the image by the camera the entire vertical section of the cell did not show in the photographs.

(2) Using a 12X magnification jeweler's loop and a precision machine divided steel scale with half millimeter divisions the magnification factor, g, was determined. This factor was determined by dividing the measured width of the image of the cell cavity, Y in mm., by 6.35.

(3) Using this magnification factor, the distance, W, across the interference pattern at a fixed value of the gradient of the optical path was measured. Usually the measurement was made at the base line of the image of the cell cavity where the interference pattern crossed the base line. This measurement, scaled by the magnification factor, was the value of 2ξ of equation (53) at the time, t, associated with the photograph.

(4) The scaled values of 2ξ were squared, plotted as a function of time on a large scale graph and smoothed. Smoothed values were read from the curves. Maximum error in the measured

values of W occurred at low time values, i.e. at small values of W.

In the calculations of the diffusion coefficients using equations (53) the smoothed values of 2ξ were used. Seldom was it found that a data point was far enough off of the smoothed curve that it had to be discarded. In Figure 17 the dashed lines outside of the lines representing the image of the width of the cell cavity are continuations of the interference pattern within the image of the cell cavity which indicate what the shape of the whole pattern would be in a wider cell.

Figure 18 shows a series of four of the actual interference patterns for the aqueous sucrose solution experiment, run number 1-S-2.

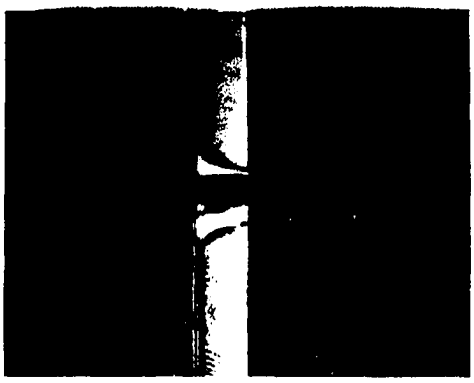

t = 4075 seconds

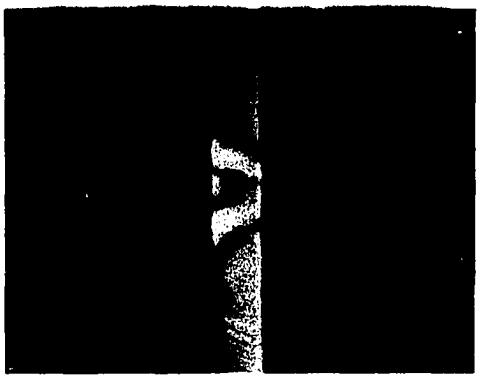

t = 11025 seconds

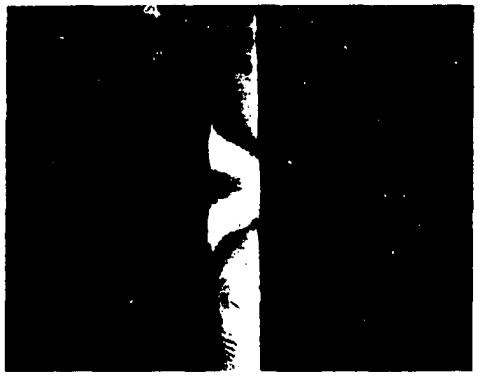

t = 14650 seconds



t = 17025 seconds

Figure 18. Interference Patterns for Various Times During Experimental Run Number 1-S-2

CHAPTER IV

EXPERIMENTAL RESULTS

Mutual diffusion coefficients were determined for 0.1 weight percent sucrose in aqueous solution at 23°C and 30°C to test the apparatus. Duplicate experiments were performed at the 23°C temperature level, one with the air circulating fan turned off and one with it on. These experiments were performed to determine if the air circulating fan caused sufficient vibration to significantly affect the results. Results of these duplicate experiments were in agreement to within one percent.

The diffusion data of Akeley and Gosting (2) and Gosting and Morris (25) on aqueous sucrose solutions are reputed to be the most accurate data in the literature. These data were determined using a Guoy interferometer and a capillary withdrawal cell. For determination of the mutual diffusion coefficient at a temperature of 25°C, for sucrose concentrations below 0.05 moles per liter of solution, Akeley and Gosting present the equation

$$D_{AB} \times 10^5 = 0.5228 - 0.2648\bar{C}_A \qquad (56)$$

where $\overline{C}_A$ is the mean concentration of sucrose in moles per liter of aqueous solution. $\overline{C}_A$ is defined by

$$\overline{C}_A = \frac{C_{A0} + C_{A1}}{2} \tag{57}$$

where C_{A0} and C_{A1} are the molar concentrations of sucrose in the less dense and more dense solutions used in the experiments. Using equation (56) and the Stokes-Einstein relationship the data of Akeley and Gosting were corrected to the temperature of the experiments reported here. The results reported here compare to within two percent of those reported by Akeley and Gosting. Results of this study and of this comparison are listed in Table 1.

Following the testing of the sucrose solutions, mutual diffusion coefficients for the triethylene glycol-water system were determined as functions of composition at temperatures of 30°C, 45°C and 65°C. Results are shown graphically in Figure 19 and are listed in Table 2.

The diffusion coefficient determined at 30°C for the 0.005 weight fraction triethylene glycol solution was compared to the predicted diffusion coefficient calculated from the Othmer-Thakar correlation, equation (33). The experimental value of 8.75×10^{-6} cm^2 per second, is four percent higher than the predicted value of 8.41×10^{-6} cm^2 per second. At higher temperatures the correlation is greatly in error but its use is not recommended above 30°C.

TABLE 1

MUTUAL DIFFUSION COEFFICIENTS,

SUCROSE-WATER SYSTEM

Run No.	Temperature °C	Sucrose Concentration grams/liter	$D_{AB} \times 10^6$ Cm^2/sec	
			This Study	Akeley and Gosting (2)
1-S-2*	23	1.000	4.88	4.84
1-S-3	23	1.000	4.91	4.84
1-S-4*	30	1.000	6.20	6.12

*air circulating fan on

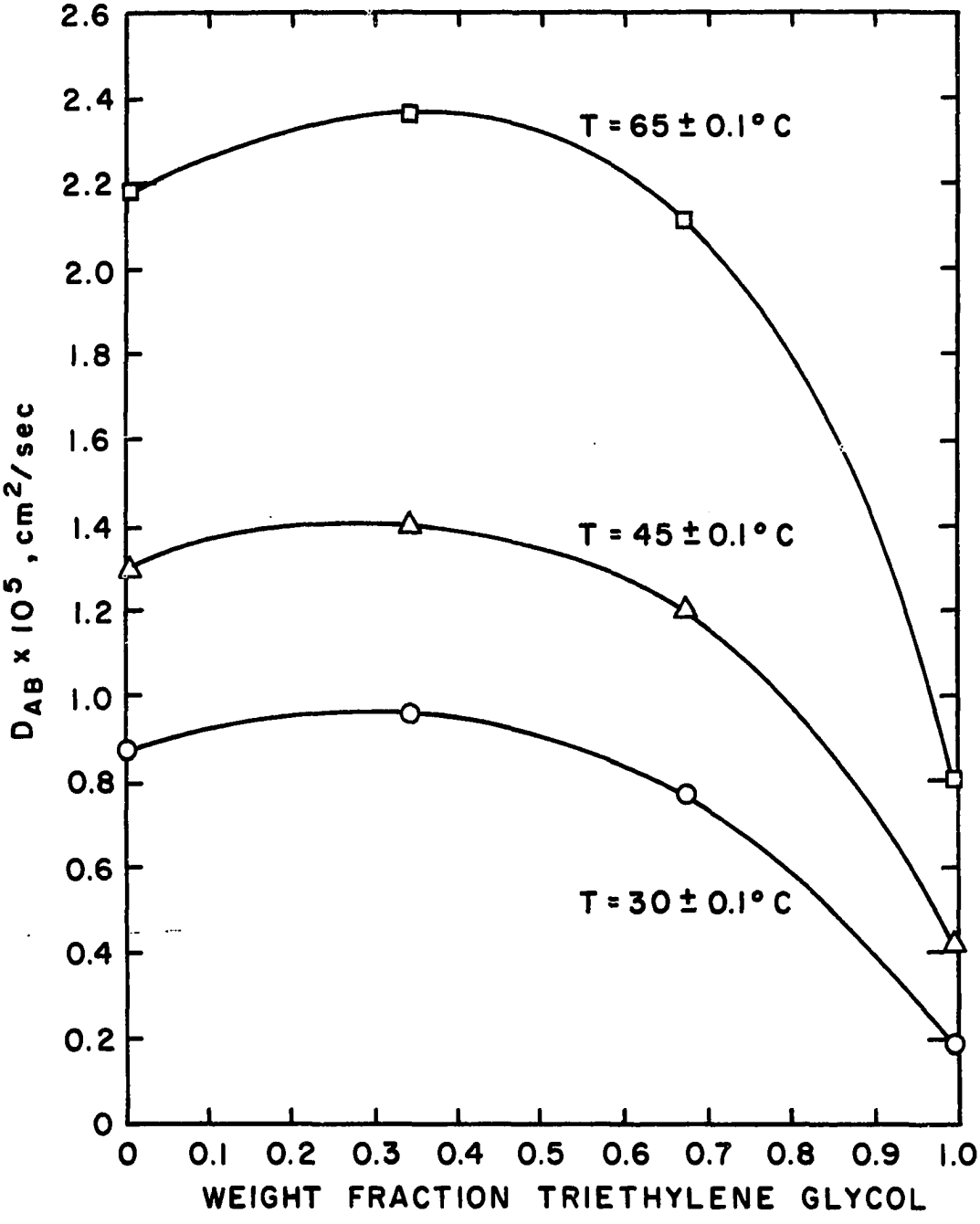

Figure 19. Molecular Diffusion Coefficients for the Triethylene Glycol-Water System as a Function of Composition and Temperature

TABLE 2

MUTUAL DIFFUSION COEFFICIENTS,

TRIETHYLENE GLYCOL-WATER SYSTEM

Run No.	Temperature °C	Weight Fraction Triethylene Glycol	$D_{AB} \times 10^5$ $Cm^2/sec.$
A-TEG-1	30	0.005	0.875
B-TEG-3	45	0.005	1.31
C-TEG-5	65	0.005	2.18
A-TEG-9	30	0.337	0.957
B-TEG-12	45	0.337	1.40
C-TEG-15	65	0.337	2.36
A-TEG-25	30	0.672	0.775
B-TEG-23	45	0.672	1.20
C-TEG-22	65	0.672	2.11
A-TEG-27	30	0.995	0.188
B-TEG-29	45	0.995	0.426
C-TEG-32	65	0.995	0.803

The diffusion coefficient determined at 30°C for the 0.995 weight fraction triethylene glycol solution was compared to the Wilke-Chang, equation (29), predicted diffusion coefficient divided by 2.3. The experimental value of 1.91×10^{-6} cm^2 per second, is 24 percent higher than the predicted value of 1.53×10^{-6} cm^2 per second. Use of the Wilke-Chang correlation is not recommended above 30°C.

Diffusion coefficients determined at 30°C were tested using the Stokes-Einstein relationship, equation (28), to correct to the higher temperatures, 45°C and 65°C. For the 0.005 weight fraction triethylene glycol solution, equation (28) predicts a diffusion coefficient that is low by 6.5 percent at 45°C and 15.4 percent low at 65°C. The diffusion coefficients predicted by equation (28) for the 0.995 weight fraction triethylene glycol solution were low by 40.3 percent and 23.3 percent at 45°C and 65°C respectively. From a theoretical point of view, equation (28) applies only to the low concentration triethylene glycol solution which accounts in part for the wide deviation at the high concentration level.

To test the Rathbun correlation, equation (42), and the correlation of Cullinan and of Vignes, equation (43), it is necessary to have activity data as a function of composition. Activity data is ordinarily determined from vapor-liquid equilibria data. No such data could be found in the literature for the triethylene glycol-water system. However,

data on the vapor pressures of triethylene glycol-water solutions as a function of composition and temperature was available (23).

This data was used with the following assumptions:

1) Due to the extremely low vapor pressure of triethylene glycol at the experimental temperatures of this study, the total vapor pressure of the solution is the vapor pressure of the water over the solution;

and 2) At the low vapor pressure of the solutions, which is less than one-third of an atmosphere at most, the vapor over the solution obeys the ideal gas law.

Activities of the water were calculated as a function of mole fraction of water in the solution. The data was curve fit to a polynomial using least squares. Best fit of the data was an equation relating activity of the water to a fifth degree polynomial in water mole fraction. No data was available to determine the activity at mole fractions of water above 0.96 or below 0.10. These points represent weight fractions of 0.752 and 0.013 respectively.

To obtain the infinite dilution diffusion coefficients needed in these correlations each of the curves in Figure 19 was extrapolated to zero water concentration and to zero triethylene glycol concentration.

Triethylene glycol-water solutions deviate negatively from Raoult's law. Therefore the exponent S in equation (42)

was taken to be 0.3 as specified by Rathbun for use in his correlation.

In Figure 20 the solid line represents the Rathbun correlation over the range of concentrations for which activity data could be calculated. It can be seen that the diffusion coefficients determined experimentally are correlated to within about five percent over this concentration range.

For the triethylene glycol-water system the correlation of Rathbun predicts diffusion coefficients that are generally higher than those determined experimentally. In an attempt to force a better fit of the curves of Figure 19 with equation (42), the exponent S was varied over the range from 0.1 to 0.3. It was found that varying S over this range had little effect on the diffusion coefficients predicted by equation (42).

The correlation of Vignes and of Cullinan, equation (43), failed to give even a semblance of agreement with the diffusion coefficients determined experimentally. Equation (43) was expressly restricted to nonassociating liquids when derived. However, data on acetone-water and ethanol water systems, published by Vignes (65), were correlated well by equation (43) indicating it might have at least limited application in associating systems.

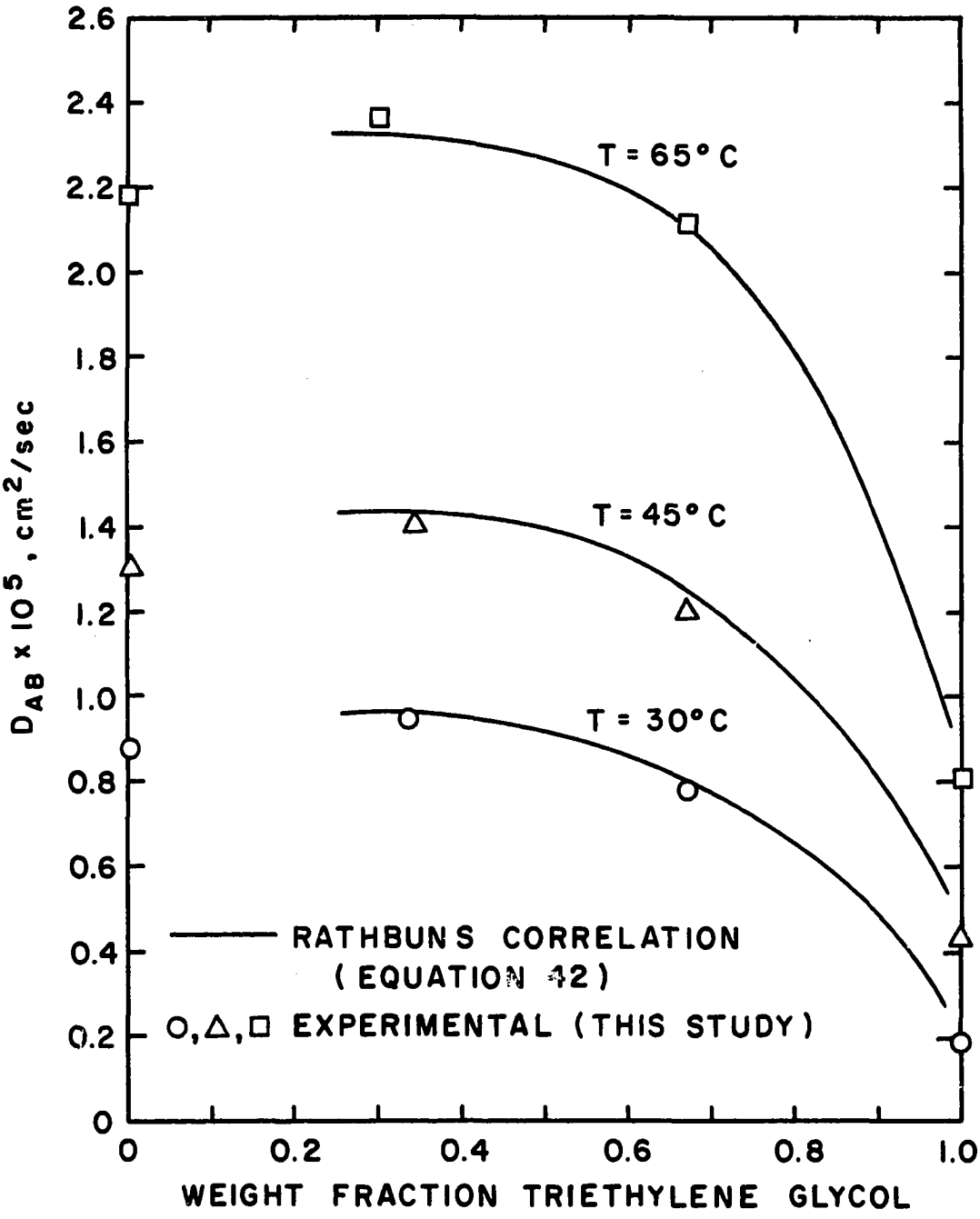

Figure 20. Comparison of Experimental Values of Diffusion Coefficients for the Triethylene Glycol-Water System to Predicted Values by Equation (42)

CHAPTER V

CONCLUSIONS AND RECOMMENDATIONS

It is concluded as a result of this research that:

(1) The experimental apparatus as used in this study was found to be capable of yielding data from which molecular diffusion coefficients could be determined to a precision of one percent or less.

(2) Due to lack of sharpness of the interference patterns recorded in the course of the experimental work, full potential of this method for determining molecular diffusion coefficients has not been realized.

(3) Modifications to the present interferometer would increase the precision of the method to less than 0.1 percent.

(4) Concentration differences on the order of only 0.1 percent by weight could be used and thereby increase the precision of determination of molecular diffusion coefficients.

(5) Greater accuracy of results could be obtained, with much greater ease, by extending the length

of the experiments to cover a greater part of the history of the diffusion experiments.

(6) Results determined for aqueous sucrose solutions by the methods used in this study compared to within two percent of the results obtained by Akeley and Gosting who used the Guoy interferometer.

(7) Molecular diffusion coefficients for the triethylene glycol-water system as a function of composition were determined to an accuracy of two percent.

(8) The Othmer-Thakar correlation was found to be reliable to within five percent in predicting the molecular diffusion coefficient for very dilute solutions of triethylene glycol in water at 30°C but failed at higher temperatures.

(9) Using the Wilke-Chang correlation, predictions of molecular diffusion coefficients for dilute solutions of water in triethylene glycol at 30°C are high by approximately 25 percent and deviate even more at higher temperatures.

(10) Using extrapolated values of the diffusion coefficients determined in this study for the infinite diffusion coefficients of the triethylene glycol-water system, the Rathbun correlation predicts the concentration dependence

of the molecular diffusion coefficients, to within 5 percent, over the range of concentrations where activity data could be determined.

(11) For the triethylene glycol-water system the correlation of Rathbun is relatively insensitive to variations in the exponent, S, of the thermodynamic factor, for values of S between 0.1 and 0.3.

To improve the accuracy and precision of results obtained with this apparatus it is recommended that

(1) The laser light source used in this study be replaced with a light source having five to ten times the intensity of the laser, to increase the sharpness of the interference patterns, or

(2) modifications be made in the lens system of the interferometer so that the laser beam illuminates only 1/2 to one inch above and below the cell slits which locate the initial boundary in the cell.

(3) A long variable extension tube of the telescoping type be constructed for the camera to replace the present lens extension system to allow for easier focusing and for greater enlargement of the interference patterns.

(4) Focusing lens L_4 (see Figure 3) be replaced with a lens of focal length approximately 1/4

of that of the present L_4 to increase the sharpness and clarity of the interference patterns.

(5) The thermocouples used to measure temperatures in this study be replaced by platinum resistance thermometers to take full advantage of the excellent temperature control which the temperature control system and constant temperature air bath afford.

LITERATURE CITED

(1) Adamson, A. W., J. W. Cobble, and J. M. Nielson, Jour. Phys. Chem., 47, 740 (1949).

(2) Akeley, D. F., and L. J. Gosting, Jour. Amer. Chem. Soc., 75, 5685 (1953).

(3) Anderson, D. K., J. R. Hall, and A. L. Babb, Jour. Phys. Chem., 62, 404 (1958).

(4) Bearman, Richard J., Jour. of Chem. Phys., 32, 1308 (1960).

(5) Bearman, Richard J., Jour. Phys. Chem., 65, 1961 (1961).

(6) Bird, R. B., Advances in Chemical Engineering, 1, 153 (1956).

(7) Bird, R. B., W. E. Stewart, and E. N. Lightfoot, Transport Phenomena, John Wiley and Sons, New York (1960).

(8) Bryngdahl, Olof, Acta Chemica Scandinavica, 11, 1017 (1957).

(9) Bryngdahl, Olof, ibid., 12, 684 (1958).

(10) Bryngdahl, Olof, and Stig Ljunggren, Jour. Phys. Chem., 64, 1264 (1960).

(11) Caldwell, C. S., J. R. Hall, and A. L. Babb, Rev. Sci. Instr., 28, 816 (1957).

(12) Calvert, E., and R. Chevalerias, Jour. Chim. Phys., 43, 37 (1946).

(13) Claesson, H., Nature, 158, 834 (1946).

(14) Creeth, J. M., Jour. Amer. Chem. Soc., 77, 6428 (1955).

(15) Cullinan, Harry T., Jr., I. and E. C. Fundamentals, 5, No. 2, 281 (1966).

(16) Darken, L. S., Trans. Amer. Inst. Min. (Metall.) Engrs., 175, 184 (1948).

(17) Fick, A., Annalen der Physik, 94, 59 (1855).

(18) Fujita, H., Jour. Phys. Soc. (Japan), 11, 1018 (1956).

(19) Gainer, J. L., and A. B. Metzner, A.I.Ch.E.-I.Ch.E. Symposium Series No. 6. 1965 (London: Instn. Chem. Engrs.).

(20) Garner, F. H., and P. J. Marchant, Trans. Inst. Chem. Engr. (London), 39, 397 (1961).

(21) Geddes, A. L., and R. B. Pontius, in A. Weissberger, ed., Physical Methods of Organic Chemistry, Interscience Publishers, New York (1959).

(22) Glasstone, S., K. J. Laidler, and H. Eyring, The Theory of Rate Processes, McGraw-Hill Book Company, New York (1941).

(23) Glycols, Union Carbide Corporation, New York, New York (1964).

(24) Gordon, A. R., Ann. N. Y. Acad. Sci., 46, 285 (1945).

(25) Gosting, L. J., and M. Morris, Jour. Amer. Chem. Soc., 71, 1998 (1949).

(26) Gosting, L. J., "Measurement and Interpretation of Diffusion," in Advances in Protein Chemistry, XI, Academic Press, New York, 429 (1956).

(27) Graham, T., Phil. Trans. Roy. Soc. (London), 140, 1, 805 (1850).

(28) Harned, H. S., and D. M. French, Ann. N. Y. Acad. Sci., 46, 267 (1945).

(29) Harned, H. S., and R. L. Nuttall, Jour. Amer. Chem. Soc. 69, 736 (1947).

(30) Hartley, G. S., and J. Crank, Trans. Faraday Soc., 45, 801 (1949).

(31) Hirschfelder, J. O., C. F. Curtiss, and R. B. Bird, Molecular Theory of Gases and Liquids, John Wiley & Sons, Inc., New York, 1954.

(32) Inglestam, E., Arkiv Fysiks, 9, 197 (1955).

(33) Inglestam, E., Jour. Opt. Soc. Amer., 47, 536 (1957).

(34) Innes, K. K., and L. F. Albright, I. and E. C., 49, 1793 (1957).

(35) Kahn, D. S., and A. Polson, Jour. Phys. Colloid Chem., 51, 816 (1947).

(36) Kamal, M. R., and L. N. Canjar, Chem. Engr., Dec. 10, 1962, pp 159.

(37) Kamal, M. R., and L. N. Canjar, A.I.Ch.E. Jour. 8, 329 (1962).

(38) Kegeles, G., and L. J. Gosting, Jour. Amer. Chem. Soc., 69, 2516 (1947).

(39) Lamm, O., Nova Acta Regiae Soc. Sci. Upsaliensis, 10, (1937) No. 6.

(40) Lewis, J. B., Jour. Appl. Chem. (London), 5, 228 (1955).

(41) Li, J. C. M., and P. Chang, Chemical Physics, 23, 518 (1955).

(42) Lightfoot, E. N., and Cussler, E. L., Jr., "Selected Topics in Transport Phenomena," Chemical Engineering Symposium Series No. 58, 61, 66 (1965).

(43) Longsworth, L. G., Jour. Amer. Chem. Soc., 69, 2510 (1947).

(44) Longsworth, L. G., Rev. Sci. Instr., 21, 524 (1950).

(45) Mehl, J. W., and G. L. A. Schmidt, Univ. of Cal. Publ. Phys., 8, 165 (1937).

(46) Mills, R., Jour. Amer. Chem. Soc., 77, 6116 (1955).

(47) Mills, R., and A. W. Adamson, Jour. Amer. Chem. Soc., 77, 3454 (1955).

(48) Mrazek, R. V., and H. C. VanNess, A. I. Ch. E. Journal, 7, 190 (1961).

(49) Neurath, H., Science, 93, 431 (1941).

(50) Northrup, J. H., and M. L. Anson, Jour. Gen. Physiol., 12, 543 (1929).

(51) Othmer, D. F., and M. S. Thakar, I. and E. C., 45, 589 (1953).

(52) Philpot, J. St. L., and G. H. Cook, Research, 1, 234 (1948).

(53) Polson, A., Jour. Phys. Colloid Chem., 54, 649 (1950).

(54) Rathbun, R. E., Ph.D. Thesis, University of Washington, Seattle, Wash., 1965.

(55) Reid, R. C., and T. K. Sherwood, The Properties of Gases and Liquids, 2nd ed., McGraw-Hill, New York (1966).

(56) Scheibel, E. G., I. and E. C., 46, 2007 (1954).

(57) Skinner, Richard D., Masters Thesis, Oklahoma State University, Stillwater, Oklahoma 1964.

(58) Stokes, R. H., Jour. Amer. Chem. Soc., 72, 763 (1950).

(59) Svensson, H., Acta Chem. Scand., 3, 1170 (1949).

(60) Svensson, H., ibid., 4, 1329 (1950).

(61) Svensson, H., Optica Acta, 1, 25 (1954).

(62) Svensson, H., Optica Acta, 3, 164 (1956).

(63) Trimble, L. E., D. Finn, and A. Cosgarea, Acta Metallurgica, 13, 501 (1965).

(64) Tyrrell, H. J. V., J. Chem. Educ., 41, 397 (1964).

(65) Vignes, Alain, I. and E. C. Fundamentals, 5, No. 2, 189 (1966).

(66) Wilke, C. R., and P. Chang, A.I.Ch.E. Jour., 1, 264 (1955).

APPENDIX A

NOMENCLATURE

a	activity
a_A	activity of component A in binary solution
A	component of binary solution
b	molecular radius in Equation 26
B	component of binary solution
C	total concentration, moles per unit volume of solution
C_i	concentration of component i, moles of i per unit volume of solution
$\overline{C}_A$	average concentration of A, defined by Equation 57
C_{AO}	concentration of component A in less dense solution
C_{Al}	concentration of component A in more dense solution
D_{AB}	Fick's mutual diffusion coefficient
D'_{AB}	pseudo diffusion coefficient defined by Equation 54
D_{ij}^{M}	mutual diffusivity relative to the local center of moles
D_{ij}^{m}	mutual diffusivity relative to the local center of mass
D_{ij}^{∞}	mutual diffusivity at infinite dilution of component i
D_{ij}^{*}	tracer diffusivity of dilute component i in component j
D_{ii}	self diffusion coefficient of component i

$E_{\mu,i}$ activation energy for viscosity of component i

$E_{D,ij}$ activation energy for diffusion for component i in component j.

$$\text{erf } y = \int_0^y e^{-y^2} dy$$

g photographic magnification factor

J_i diffusional flux of component i from Fick's first law

J_i^M diffusional flux of component i relative to the local center of moles

ΔH_i latent heat of vaporization of component i

k Boltzmann's constant

k_o constant defined by Equation 48

k_1 constant defined by Equation 48

K constant in Scheibel equation, defined by Equation 28

K_1 factor in Kamal-Canjar equation

K_2 factor in Kamal-Canjar equation

L lens

M_i molecular weight of component i

n refractive index

N_o Avogadros number

p summation index

Q volumetric flow rate

R gas law constant

S Savart plate

T absolute temperature

t time variable

t' translated time defined by Equations B-8 and B-9

u_i velocity of component i relative to fixed axes

u^m velocity of the local center of mass relative to fixed axes

u^M velocity of the local center of moles relative to fixed axes

V_c volume of test cell chamber

$\underline{V}_i$ specific volume of component i, volume per mole

$\overline{V}_i$ partial molal volume of component i in solution, volume per mole

W measurement parameter from photographic data

X_i mole fraction of component i in solution

Y width of the cell cavity in photographs, mm.

Z optical path length

Greek letters

α cell thickness in line of optical path

β calibration constant

γ time translation factor defined by Equations B-8, B-9 and B-10

δ geometrical configuration parameter defined by Equation 34

θ time factor defined by Equation 55

μ_i viscosity of component i

ξ distance coordinate in one dimensional linear diffusion systems

ρ mass density of solution

ρ_i mass density of component i in binary solution, mass of i per unit volume of solution

Φ association parameter in Wilke-Chang equation

ω_i weight fraction of component i in solution

APPENDIX B

MATHEMATICAL DERIVATIONS

Derivation of Equations (53), (54) and (55)

Equation (53) was involved in the zero time correction of the initial boundary condition between the two fluids in the test cell.

The imperfection of the initial boundary can be characterized by a time correction, Δt, applied to the measured time in the experiment. Equation (52), in the text, was derived on the assumption of a perfect interface at time zero. Beginning with equation (52) the time correction was made mathematically as

$$D_{AB} = \frac{\dfrac{(2\xi_i)^2}{t_i + \Delta t} - \dfrac{(2\xi_j)^2}{t_j + \Delta t}}{8 \ln \dfrac{t_j + \Delta t}{t_i + \Delta t}} \qquad \text{(B-1)}$$

Defining

$$R = \left(\frac{\xi_j}{\xi_i}\right)^2 \qquad \text{(B-2)}$$

and taking $t_j > t_i$, equation (B-1) may be rewritten

$$D_{AB} = \frac{(2\xi_i)^2 \left\{ \frac{t_j - Rt_i - \Delta t(R-1)}{t_i t_j + \Delta t(t_i + t_j) + (\Delta t)^2} \right\}^2}{8 \ln \frac{t_j + \Delta t}{t_i + \Delta t}} \quad \text{(B-3)}$$

Series expansion of the logarithmic term in (B-3) gives

$$\ln \frac{t_j + \Delta t}{t_i + \Delta t} = \ln \frac{t_j}{t_i} + \sum_{p=1}^{\infty} (-1)^p \left\{ \left(\frac{\Delta t}{t_i} \right)^p - \left(\frac{\Delta t}{t_j} \right)^p \right\} \quad \text{(B-4)}$$

Substituting (B-4) into (B-3) and rearranging results in

$$D_{AB} = \frac{(2\xi_i)^2 \left\{ \frac{t_j - Rt_i}{t_i t_j} - \frac{\Delta t(R-1)}{t_i t_j} \right\}}{8 \ln \frac{t_j}{t_i} \left\{ 1 + \frac{\Delta t(t_i + t_j) + (\Delta t)^2}{t_i t_j} \right\} \left\{ 1 + \frac{\sum_{p=1}^{\infty} (-1)^p \left[\left(\frac{\Delta t}{t_i} \right)^p - \left(\frac{\Delta t}{t_j} \right)^p \right]}{\ln \frac{t_j}{t_i}} \right\}} \quad \text{(B-5)}$$

For $R\Delta t \ll t_i$ equation (B-5) reduces to

$$D_{AB} \approx \frac{(2\xi_i)^2 \left(\frac{1}{t_i} - \frac{R}{t_j} \right)}{8 \ln \frac{t_j}{t_i} \left\{ 1 + \Delta t \left(\frac{t_i + t_j}{t_i t_j} \right) \right\} \left\{ 1 - \Delta t \left(\frac{\frac{1}{t_i} - \frac{1}{t_j}}{\ln \frac{t_j}{t_i}} \right) \right\}} \quad \text{(B-6)}$$

which becomes, on dropping the second and higher order Δt terms and multiplying out the numerator,

$$D_{AB} \approx \frac{\frac{(2\xi_i)^2}{t_i} - \frac{(2\xi_j)^2}{t_j}}{8\left\{\ln \frac{t_j}{t_i}\right\}\left\{1 + \Delta t\left(\frac{t_i + t_j}{t_i t_j} - \frac{\frac{1}{t_i} - \frac{1}{t_j}}{\ln \frac{t_j}{t_i}}\right)\right\}} \quad . \tag{B-7}$$

How closely equation (B-7) approximates D_{AB} depends upon how much error is introduced by the assumption that $R\Delta t \ll t_i$. To insure that the value of Δt was sufficiently small to validate the assumptions made in arriving at equation (B-7), new times were defined as

$$t_i' = t_i + \gamma \tag{B-8}$$

$$t_j' = t_j + \gamma \quad . \tag{B-9}$$

For these times the actual Δt in the experiment was

$$\Delta t = \gamma + \Delta t' \tag{B-10}$$

and equation (B-7) becomes

$$D_{AB} \approx \frac{D_{AB}'}{(1 + \Delta t'\theta)} \tag{B-11}$$

where

$$D'_{AB} \approx \frac{\frac{(2\xi_i)^2}{t'_i} - \frac{(2\xi_j)^2}{t'_j}}{8 \ln \frac{t'_j}{t'_i}} \qquad \text{(B-12)}$$

and

$$\theta = \frac{t'_i + t'_j}{t'_i t'_j} - \frac{\frac{1}{t'_i} - \frac{1}{t'_j}}{\ln \frac{t'_j}{t'_i}} \qquad \text{(B-13)}$$

Equations (B-11), (B-12) and (B-13) are identical to equations (53), (54) and (55) of the text.

When the value of γ in equation (B-10) is very nearly equal to the actual Δt of the experiment, a plot of D'_{AB} against θ will be a straight line with slope equal to $D_{AB}\Delta t'$ and the intercept at θ equals zero will be the value of D_{AB}. The slope of the line will be positive for γ less than the actual Δt and negative for γ greater than the actual Δt. For values of γ much less or much greater than the actual Δt the line will have positive or negative curvature.

Equations (B-12) and (B-13) were evaluated for various values of γ taken on ten second intervals. Plots were made of D'_{AB} against θ and the resulting straight line with least slope was extrapolated to θ equals zero to determine D_{AB}.

APPENDIX C

GRAPHS OF CALCULATED DATA

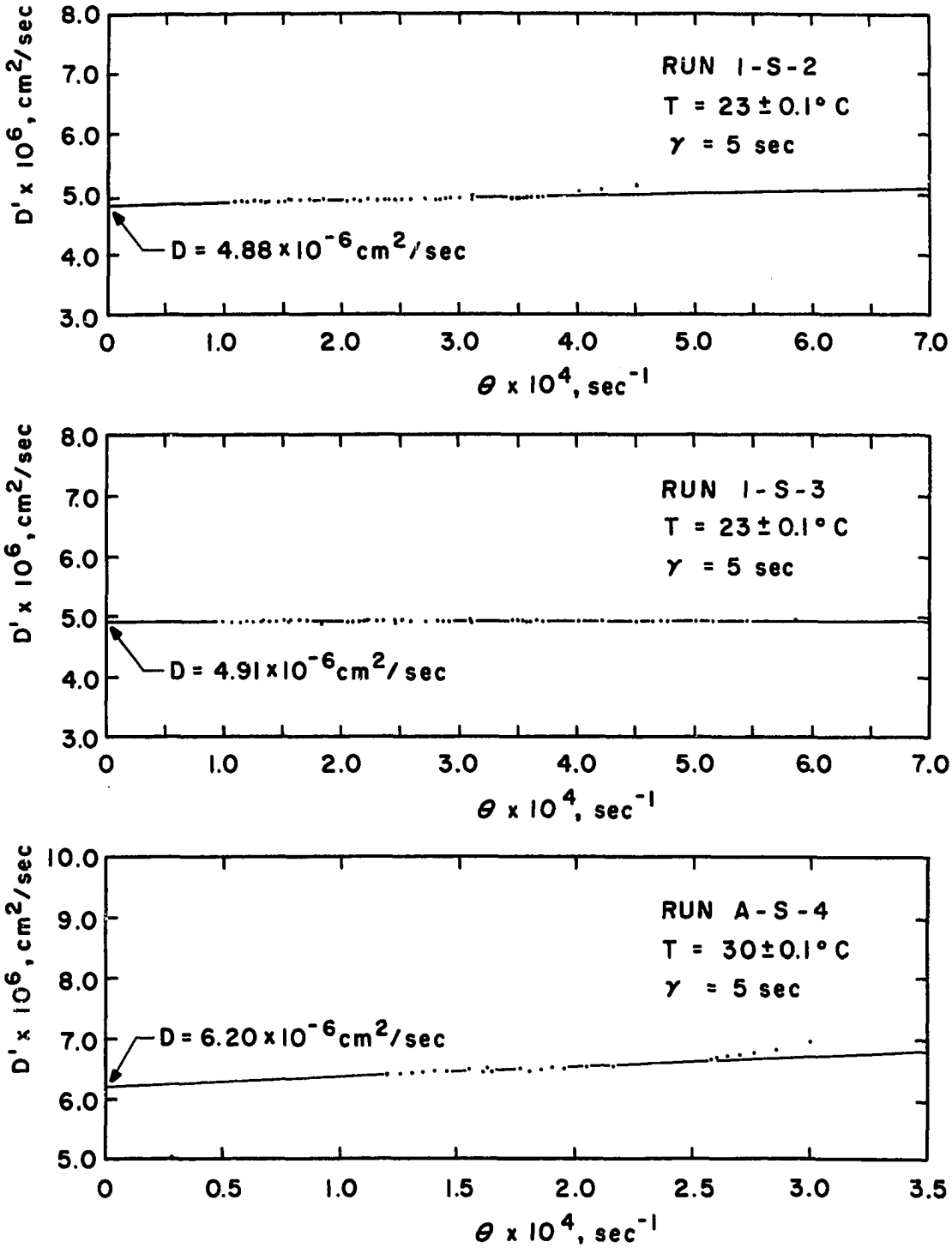

Figure 12. Determination of the Diffusion Coefficient from D'_{AB} and θ for 0.1 Weight Percent Aqueous Sucrose Solution

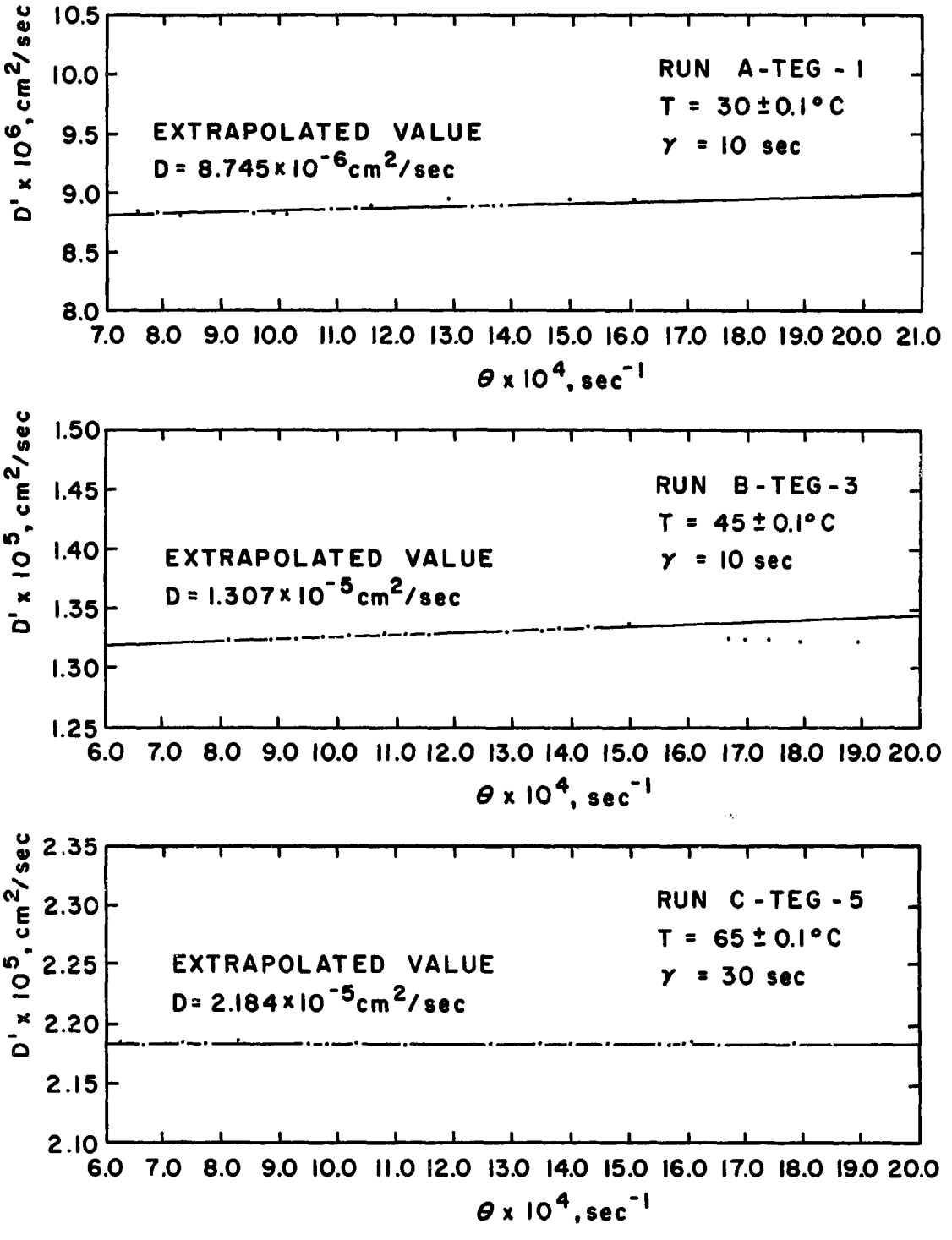

Figure 13. Determination of the Diffusion Coefficient from D'_{AB} and θ for 0.5 Weight Percent Triethylene Glycol-Water Solution

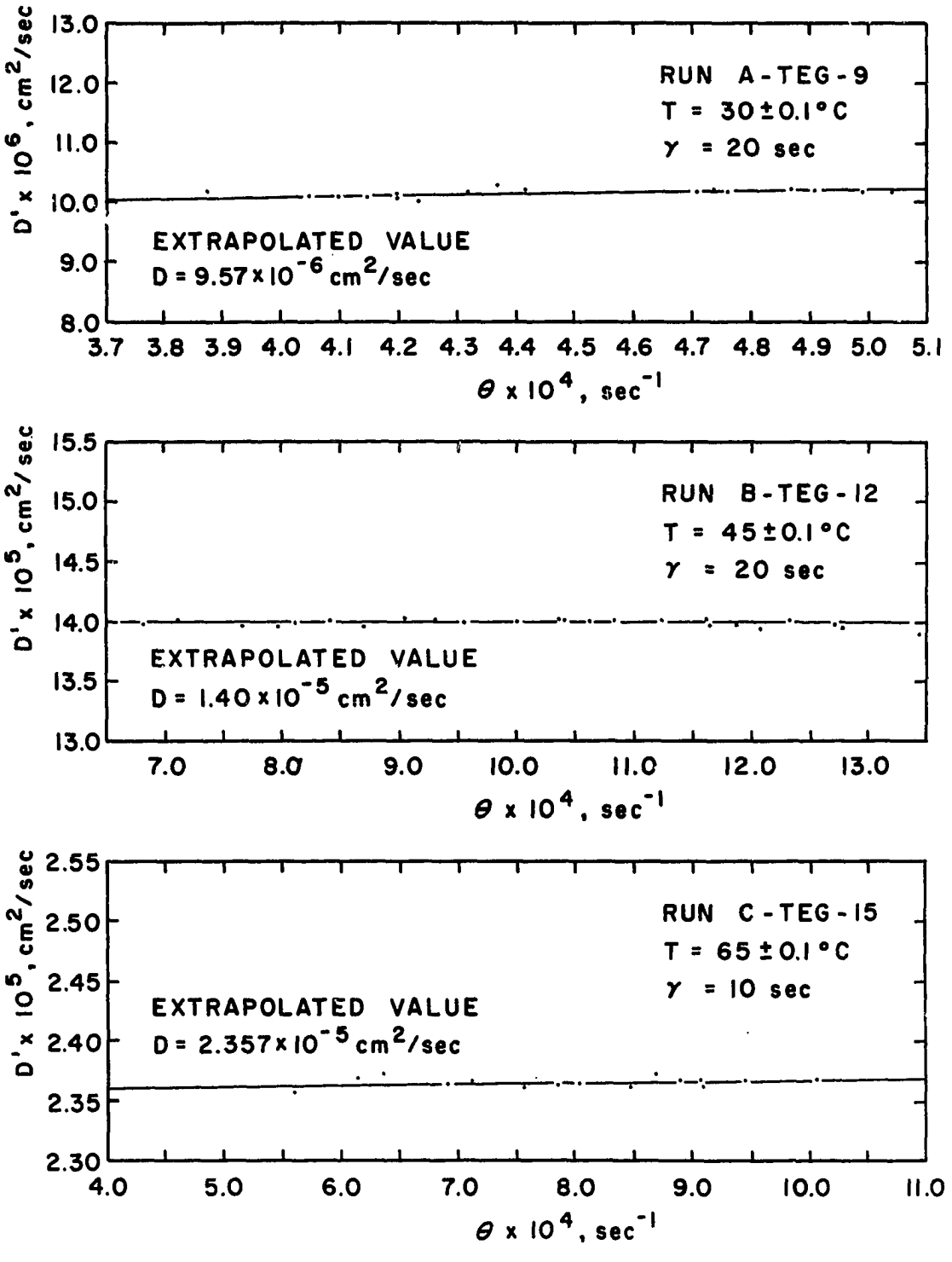

Figure 14. Determination of the Diffusion Coefficient from D'_{AB} and θ for 34 Weight Percent Triethylene Glycol-Water Solution

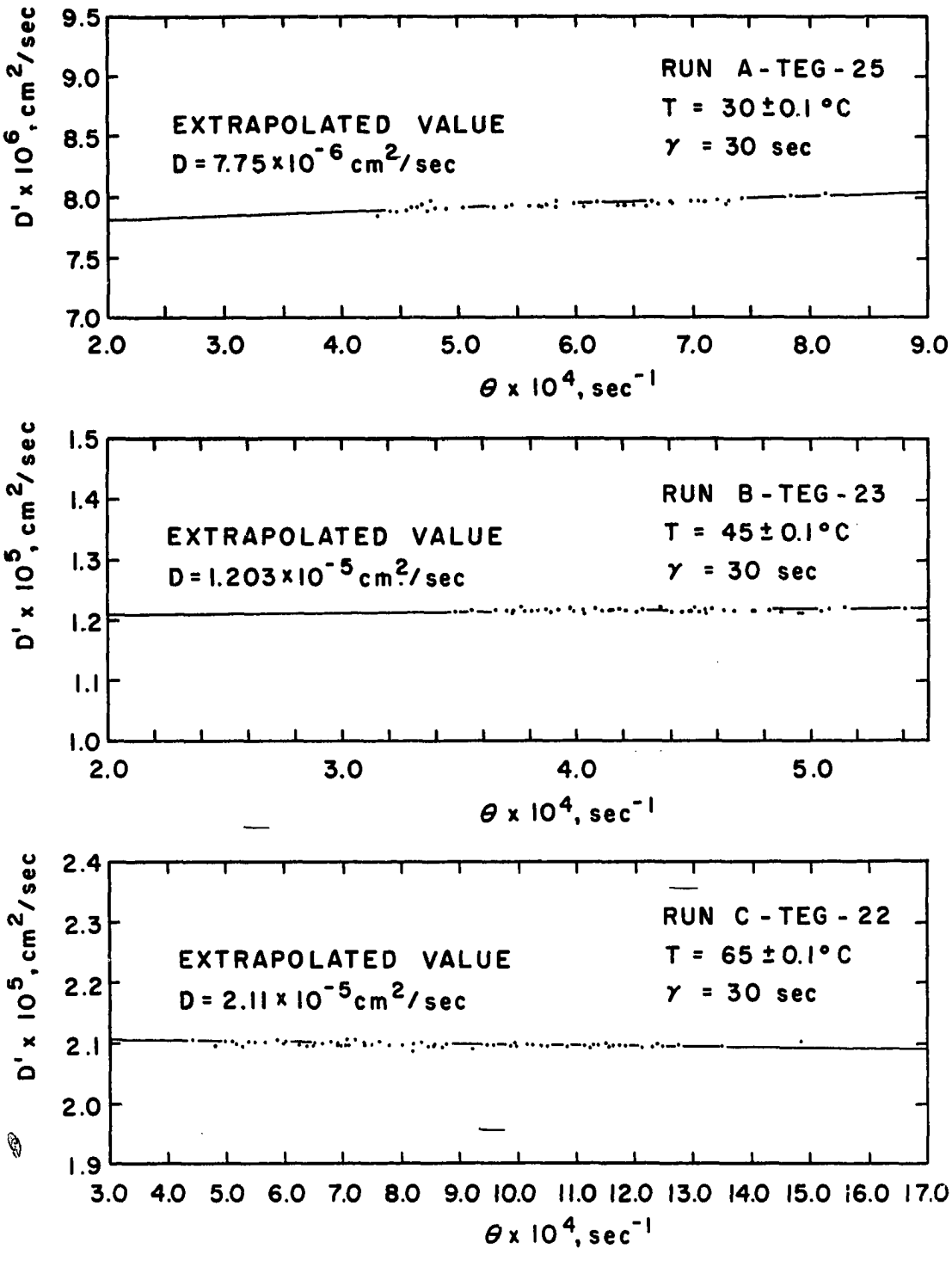

Figure 15. Determination of the Diffusion Coefficient from D'_{AB} and θ for 67 Weight Percent Triethylene Glycol-Water Solution

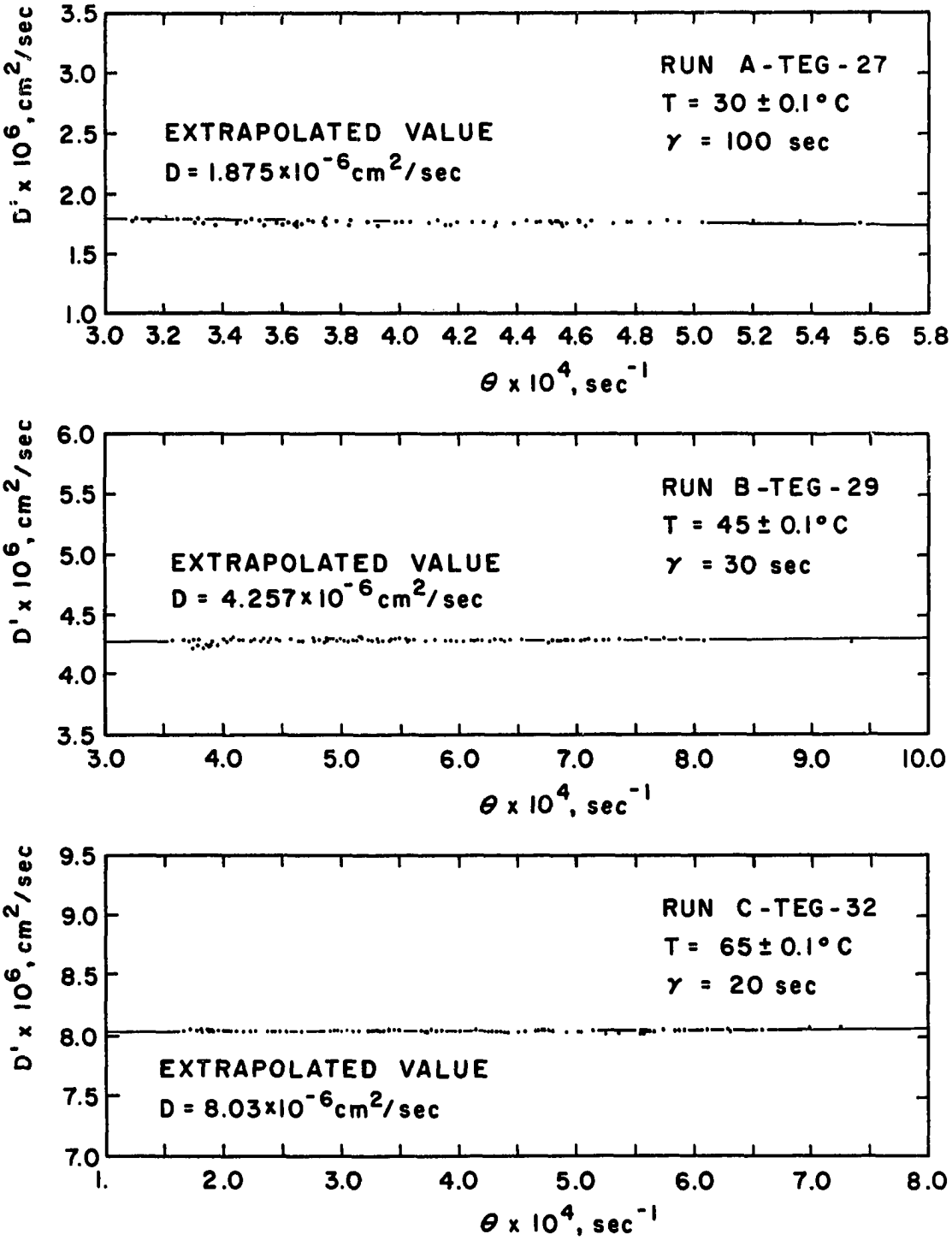

Figure 16. Determination of the Diffusion Coefficient from D'_{AB} and θ for 99.5 Weight Percent Triethylene Glycol-Water Solution